CLAS-NOTE 2003-009

A Monte Carlo study of $\gamma d \rightarrow npK^+K^-$

Curtis A. Meyer
Carnegie Mellon University
June 18, 2003

Abstract

A Monte Carlo study of the reaction $\gamma d \rightarrow K^+K^-NN_{spec}$ where one of the kaons rescatter off the spectator nucleon has been carried out. Resonance structure in both the K^-N and K^+K^- systems have been examined to look at the effect that they have on the K^+n invariant mass spectra. Resonances in combination with simple cuts seem unable to explain an extremely narrow structure in the K^+n system. It is however possible to produce a structure with a σ of $40\,MeV$.

1 Introduction

This study includes a review of known low energy kaon-nucleon scattering cross sections, current phase shift analysis results, and a Monte Carlo study of photo production reactions. The goal is to determine if it is possible to produce a narrow peak in the K^+n invariant mass spectra through a combination of known resonances and looses analysis cuts. This study does not include any detailed detector Monte Carlo and makes no effort to describe the acceptance of of any detector. Other reactions such as $K \rightarrow \mu\nu$, or K-π mis-identification are not considered here. We have also ignored Fermi-momentum in the deuteron, and have assumed that all reactions involve a primary and spectator nucleon, and that the spectator then acquires its final momentum through a rescattering off on of the final state kaons. Finally, we have ignored possible interference effects between the meson and baryon resonance systems. Under these caveats it appears very difficult to produce bumps in the K^+n spectrum that are narrower than $\sigma = 40\,MeV$.

2 Cross sections KN Scattering

There is a great deal of archived data on K-nucleon scattering. The Durham HEP Databases [1] provide archived cross section and other scattering observables for a wealth of data. In addition, the *Center for Nuclear Studies* at George Washington University maintains a data base of partial wave analysis results for many reactions [2]. In this particular study, we are worried about rescattering of both K^+ and K^- from spectator protons and neutrons in deuterium. The Ks have lab momentum from about 0 up to about $2\,GeV/c$. A rough spectrum is shown in Figure 1, as well as a mapping between laboratory kaon momentum and center-of-mass energy in the K-nucleon system. As a reference, threshold center-of-mass energy is about $1.43\,GeV/c^2$, while an energy of about $1.54\,GeV/c^2$ corresponds to a lab momentum of about $0.450\,GeV/c$.

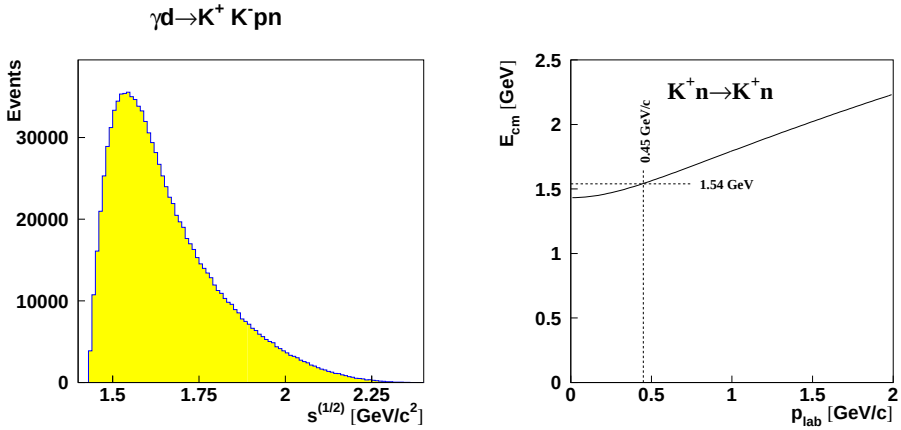

Figure 1: The center of mass energy as a function of laboratory K^+ momentum for the reaction $K^+n \rightarrow K^+n$. A mass of $1.54\,GeV/c^2$ corresponds to a laboratory momentum of about $0.45\,GeV/c$.

Using the Durham HEP database, we have extracted center-of-mass cross-section measurements, $\frac{d\sigma}{d\Omega}$ from a set of old experiments [4, 5]. Figures 6, 7, 8 and 9 show measured differential cross sections for the reaction $K^-d \rightarrow K^-n(p_{spectator})$ for kaon lab frame momenta of $612\,MeV/c$, $643\,MeV/c$, $674\,MeV/c$, $702\,MeV/c$, $730\,MeV/c$, $806\,MeV/c$, $851\,MeV/c$, $935\,MeV/c$, $1138\,MeV/c$, $1236\,MeV/c$, $1335\,MeV/c$, $1435\,MeV/c$, $1537\,MeV/c$, $1640\,MeV/c$, $1841\,MeV/c$ and $2015\,MeV/c$. Figures 3 and 4 show measured differential cross sections for the reaction $K^+d \rightarrow K^+n(p_{spectator})$ for kaon

lab frame momenta of 434 MeV/c, 526 MeV/c, 604 MeV/c, 688 MeV/c, 771 MeV/c, 853 MeV/c, and 936 MeV/c. Overlaid on top of these are the predicted differential cross sections from the SAID database [2] from the results of an analysis of the K^+N system [3]. While the agreement is not perfect, it is quite close. The cross sections in both cases are similar in magnitude at about $\frac{1\,mb}{sr}$. The K^+n cross sections are roughly isotropic, while the K^- cross sections in this energy range appear to more closely follow a $\cos^2\theta$ angular distribution.

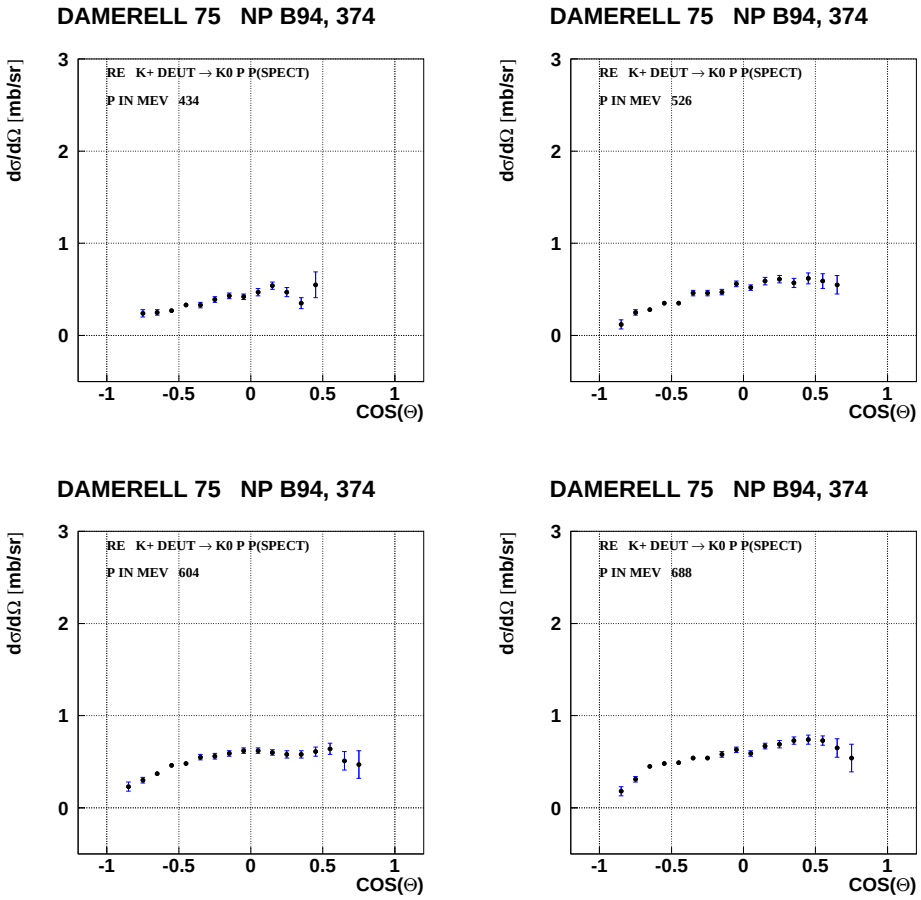

Figure 2: The differential cross section, $\frac{d\sigma}{d\Omega}$ for the reaction $K^+n \to K^0p$ as measured in the center of mass frame for four different momentum kaon beams (as measured in the lab).

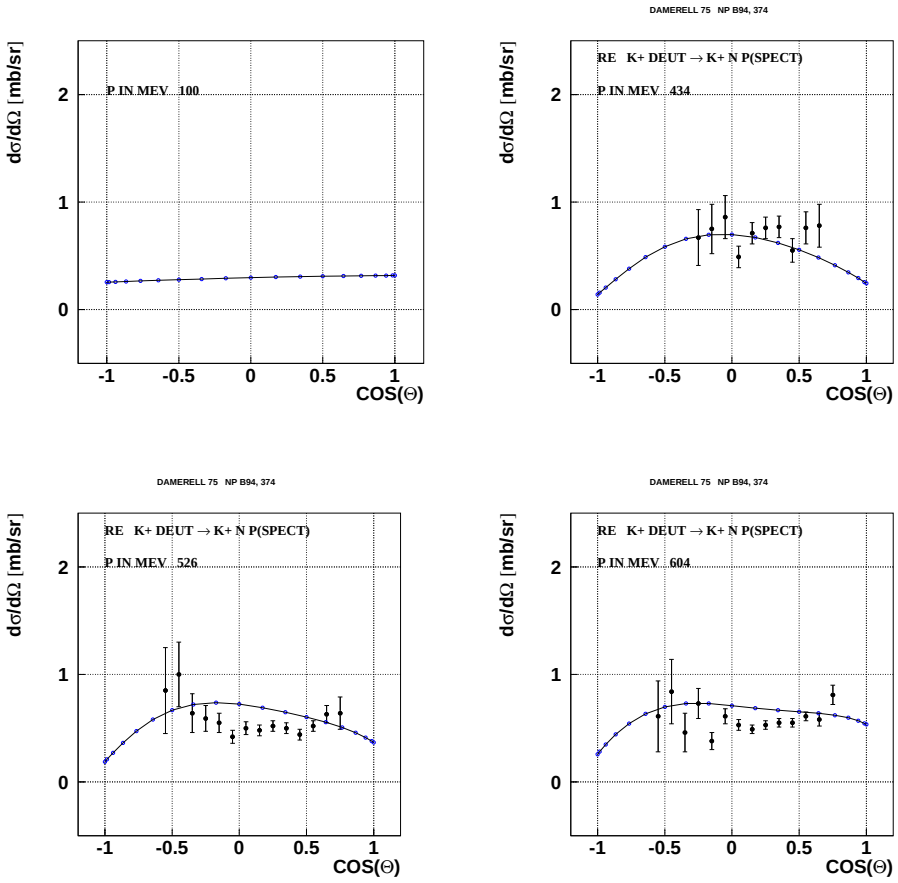

Figure 3: The differential cross section, $\frac{d\sigma}{d\Omega}$ for the reaction $K^+n \rightarrow K^+n$ as measured in the center of mass frame for four different momentum kaon beams (as measured in the lab). The data are take from reference [4], while the overlaid curve is generated from the SAID data base [2].

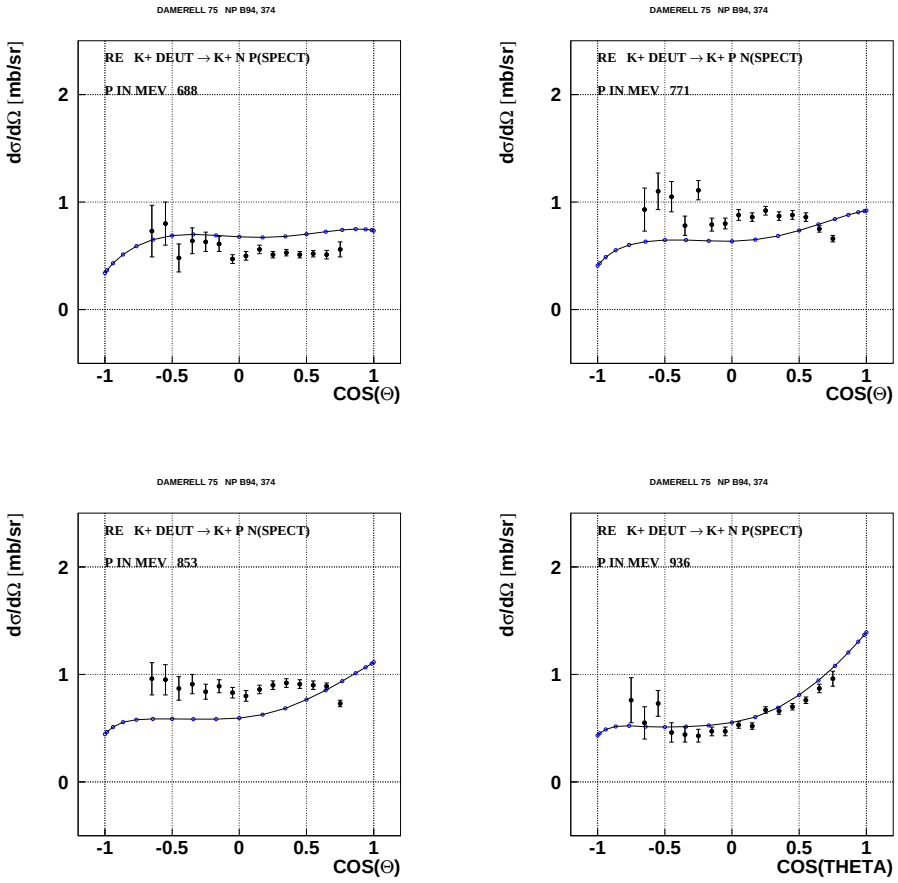

Figure 4: The differential cross section, $\frac{d\sigma}{d\Omega}$ for the reaction $K^+n \rightarrow K^+n$ as measured in the center of mass frame for three different momentum kaon beams (as measured in the lab). The data are take from reference [4], while the overlaid curve is generated from the SAID data base [2].

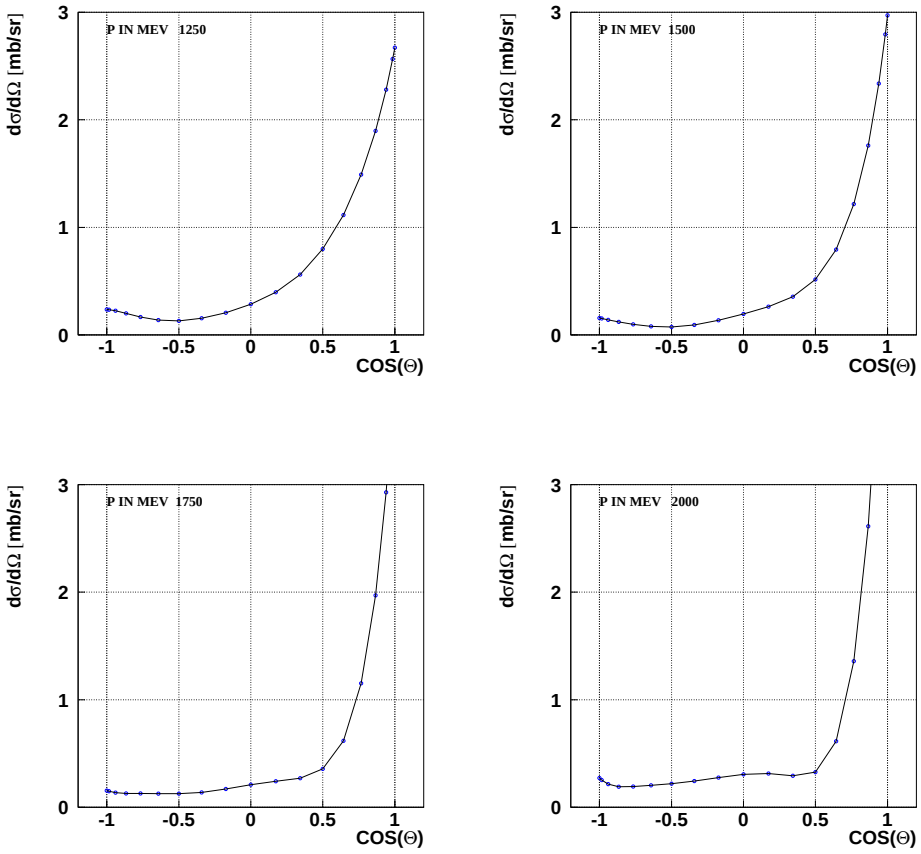

Figure 5: The differential cross section, $\frac{d\sigma}{d\Omega}$ for the reaction $K^+n \rightarrow K^+n$ as generated from the SAID data base [2].

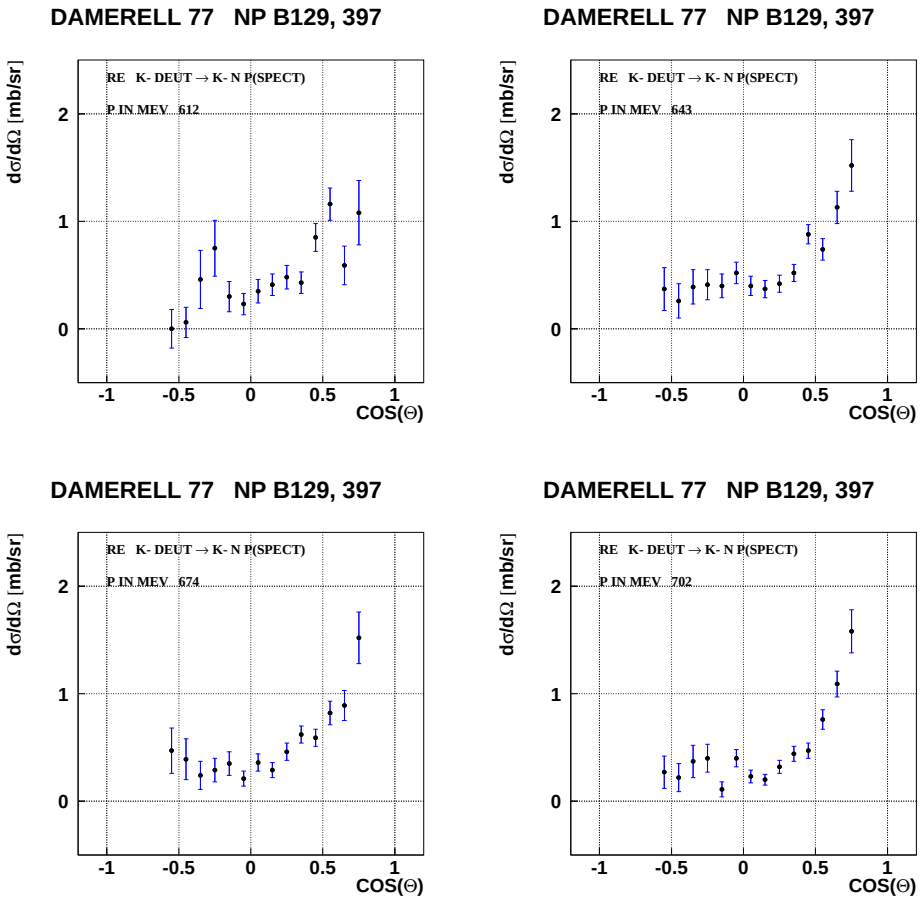

Figure 6: The differential cross section, $\frac{d\sigma}{d\Omega}$ for the reaction $K^- n \rightarrow K^- n$ as measured in the center of mass frame for three different momentum kaon beams (as measured in the lab).

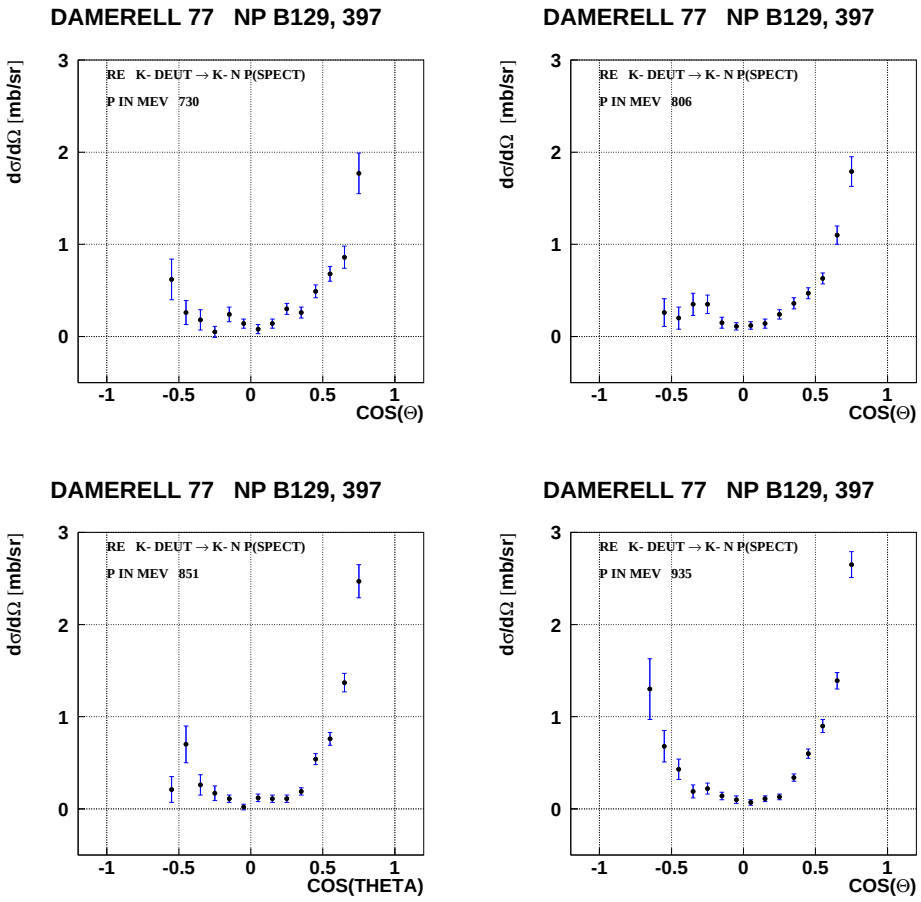

Figure 7: The differential cross section, $\frac{d\sigma}{d\Omega}$ for the reaction $K^- n \rightarrow K^- n$ as measured in the center of mass frame for three different momentum kaon beams (as measured in the lab).

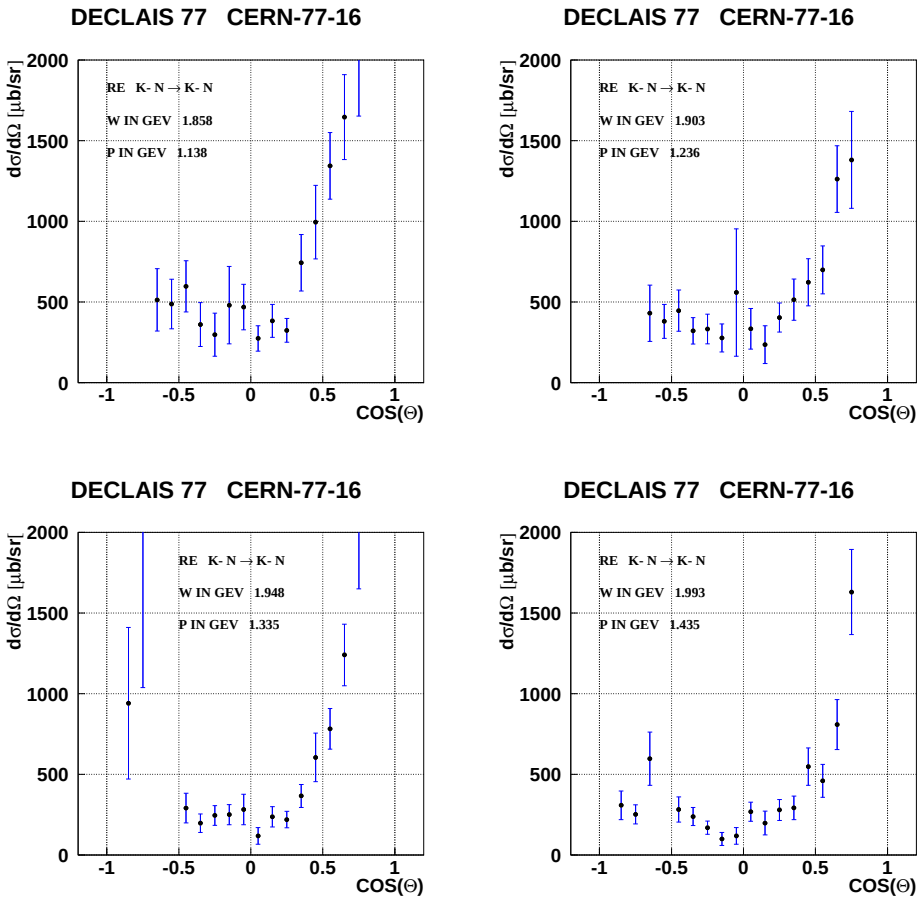

Figure 8: The differential cross section, $\frac{d\sigma}{d\Omega}$ for the reaction $K^- n \rightarrow K^- n$ as measured in the center of mass frame for three different momentum kaon beams (as measured in the lab).

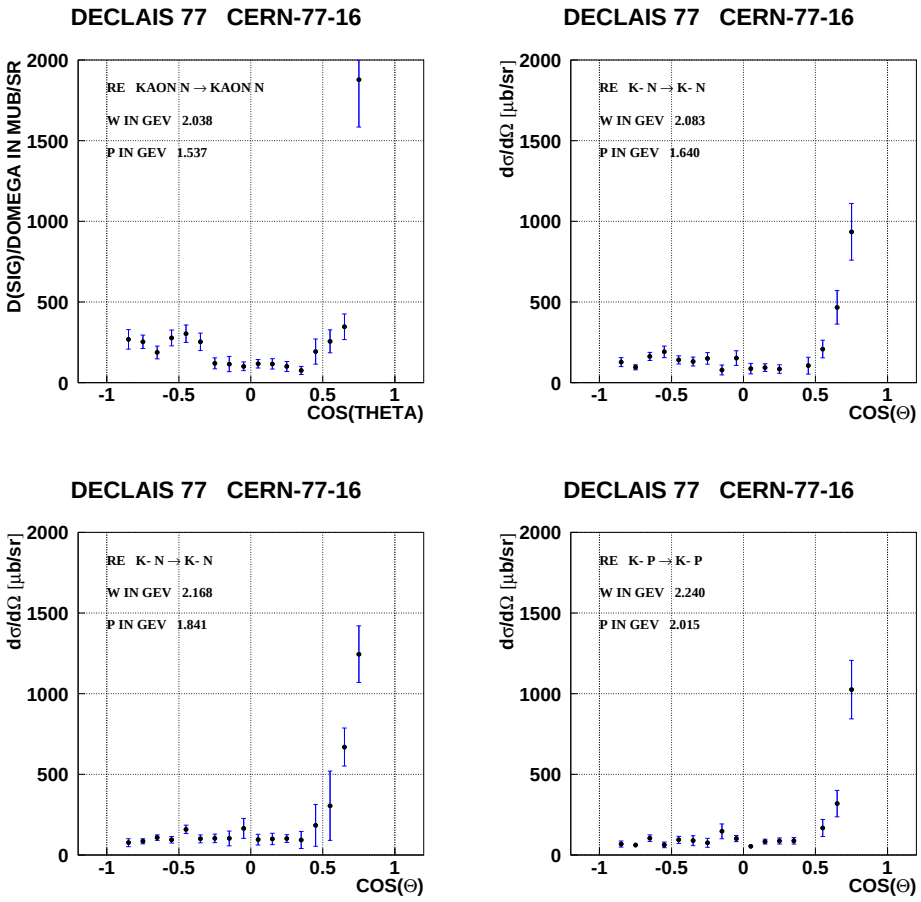

Figure 9: The differential cross section, $\frac{d\sigma}{d\Omega}$ for the reaction $K^- n \rightarrow K^- n$ as measured in the center of mass frame for three different momentum kaon beams (as measured in the lab).

3 K^+n Phase Shifts

The phase shifts for K^+n have been reported in reference [3] and can be extracted from the SAID database. The partial waves are reported using the $L_{I,2J}$ notation. For the K^+n system, isospin can be either 0 or 1. For s-wave (L=0), $J = \frac{1}{2}$. For p-wave (L=1), $J = \frac{1}{2}$ or $\frac{3}{2}$. The s-waves for both $I = 0$ and $I = 1$ are shown in figure 10. The real and imaginary parts of the T matrix (as plotted in Figures 10, 11 and 12) are related to the phase shift δ and the elasticity η via:

$$Re\,[T] = \frac{1}{2}\,(\eta \sin 2\delta) \qquad\qquad Im\,[T] = \frac{1}{2}\,(1 - \eta \cos 2\delta)$$

A negative real part of T corresponds to a negative δ, while a positive real part of T corresponds to a positive δ. Because the phase angle is negative in both cases, the interaction is repulsive. The p-wave for $J = \frac{1}{2}$ is shown in Figure 11. Here, the $I = 0$ channel appears attractive while the $I = 1$ is repulsive. Finally, Figure 12 shows the $J = \frac{3}{2}$ partial waves. Here the $I = 0$ is repulsive and the $I = 1$ is attractive. It should be pointed out that even though two of the channels are attractive, the phase never gets anywhere near 90° in the low mass regime. In fact, Figure 13 shows the P01 phase shift as a function of incident K^+ momentum. Overlaid on this is what a resonance described by a relativistic Breit-Wigner form with a mass of $1.550\,GeV/c^2$ and a width of $0.020\,GeV$ would look like. Figures 14 shows the results for a $0.010\,GeV$ and $0.005\,GeV$ width resonance. Also displayed is the difference as a dashed lines and small crosses to indicate at what momentum the measured data are. There is not a great deal of play for such a resonance to exist in the data. The resonance shape depends on the relative angular momentum, L, with which the resonance is produced. In addition, the width, $\Gamma(m)$ depends on the orbital angular momentum l between the daughter products, as well as phase space available to them. The momentum p is that of the daughter particles in the rest frame of the resonance, while p_0 is the momentum evaluated at the resonance mass, m_0.

$$\mathrm{BW}_l(m) = \frac{m_0\Gamma(m,l)}{m_0^2 - m^2 - im_0\Gamma(m,l)} \tag{1}$$

$$\Gamma(m,l) = \Gamma_0 \frac{m_0}{m}\frac{p}{p_0}\frac{F_l^2(p)}{F_l^2(p_0)} \tag{2}$$

The angular momentum barrier factors are computed as a function of $z = (p/p_R)^2$, ($p_R = 197\,\mathrm{MeV/c}$), and are given as follows:

$$F_0(p) = 1$$

$$
\begin{aligned}
F_1(p) &= \sqrt{\frac{2z}{z+1}} \\
F_2(p) &= \sqrt{\frac{13z^2}{(z-3)^2+9z}} \\
F_3(p) &= \sqrt{\frac{277z^3}{z(z-15)^2+9(2z-5)^2}}
\end{aligned}
$$

We have used $l = 0$ for the decay of the phases shift comparisons, while in reality $l = 1$ is more reasonable.

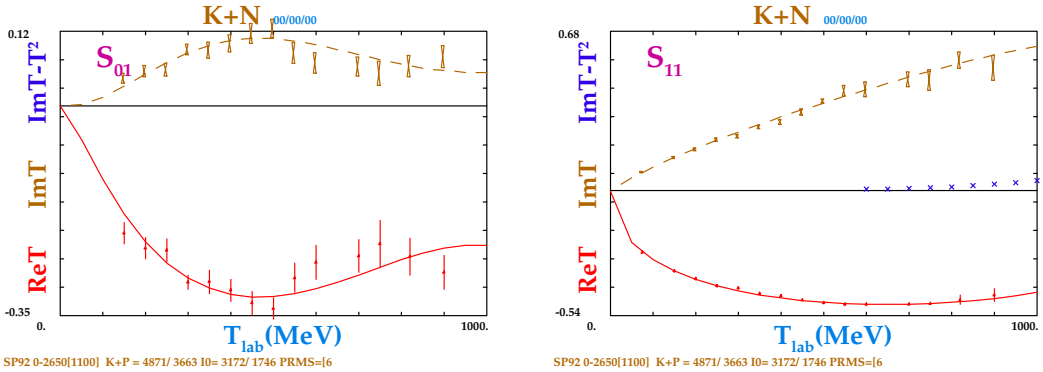

Figure 10: The S_{01} and S_{11} Scattering amplitudes.

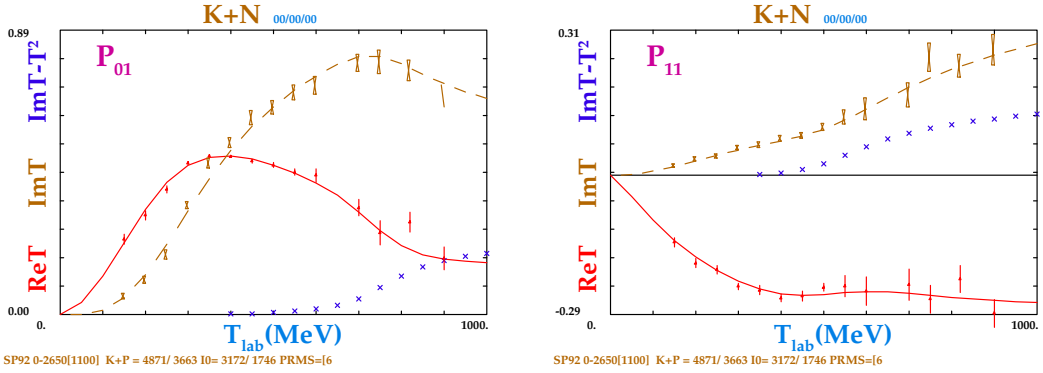

Figure 11: The P_{01} and P_{11} Scattering amplitudes.

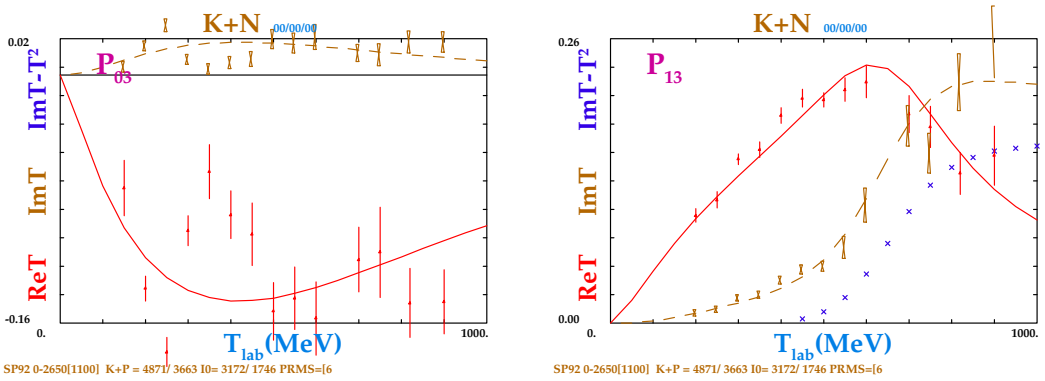

Figure 12: The P_{03} and P_{13} Scattering amplitudes.

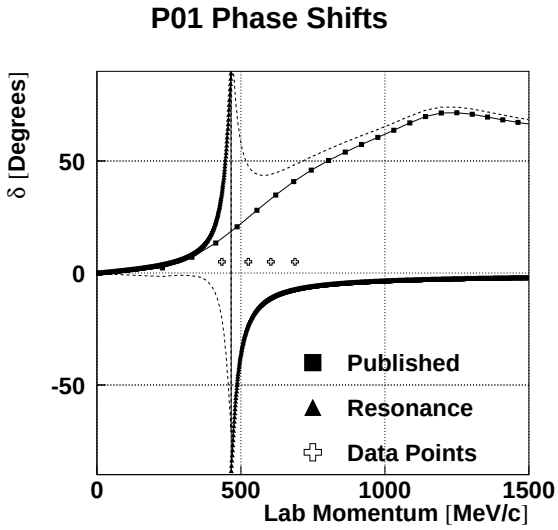

Figure 13: The published P01 phase shift, $\delta(p)$ and the expected phase shift for a Relativistic Breit-Wigner resonance with threshold effects applied. The mass and width of the resonance are $m = 1.550\,GeV/c^2$ and $\Gamma_o = 0.020\,GeV$. The dashed curve is the difference between the phase shift analysis and the resonance. The crosses represent the values of momentum at which data have been measured.

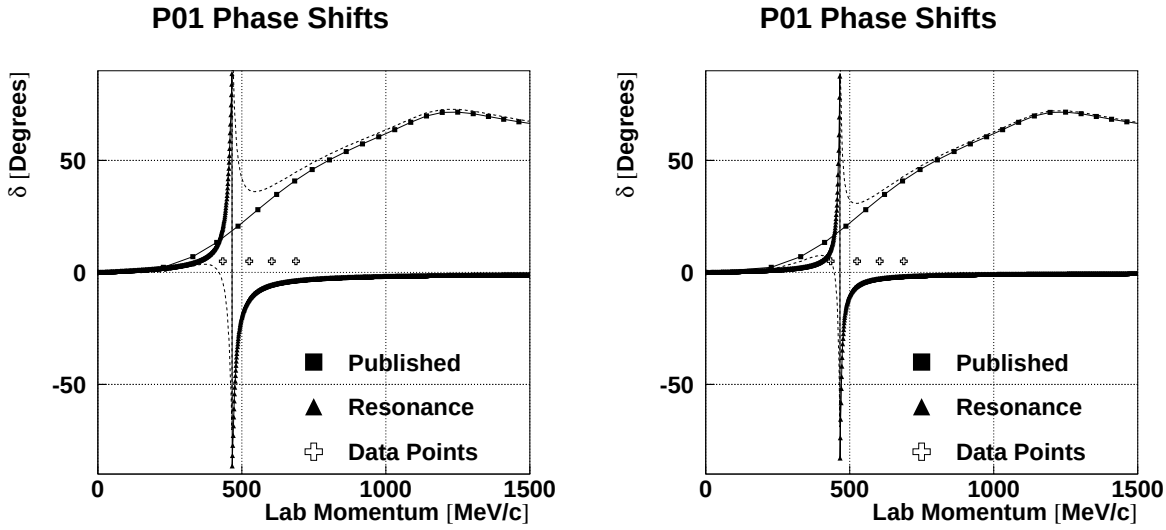

Figure 14: The published P01 phase shift, $\delta(p)$ and the expected phase shift for a Relativistic Breit-Wigner resonance with threshold effects applied. The mass of the resonance is $m = 1.550\,GeV/c^2$. The left hand figure has a width of $\Gamma_o = 0.010\,GeV$ while the right hand figure has a width of $\Gamma_o = 0.005\,GeV$. The dashed curve is the difference between the phase shift analysis and the resonance. The crosses represent the values of momentum at which data have been measured.

4 Monte Carlo Generation

Events have been generated using a phase-space Monte Carlo, GENBOD [6] using two assumed reactions, 3 and 4. In both of these, the non-struck nucleon is assumed to be a spectator and is initially at rest.

$$\gamma p \rightarrow pK^+K^- \quad (3)$$
$$\gamma n \rightarrow nK^+K^- \quad (4)$$

In a subsequent reaction, one of the kaons will rescatter off the spectator nucleon as per reactions 5,6,7 and 8.

$$K^-n \rightarrow K^-n \quad (5)$$
$$K^+n \rightarrow K^+n \quad (6)$$
$$K^-p \rightarrow K^-p \quad (7)$$
$$K^+p \rightarrow K^+p \quad (8)$$

This subsequent scatter is initially assumed to be both energy independent and isotropic in its center of mass frame. However, it is possible to weight the events using these quantities.

The events are generated using a photon beam whose energy distribution is shown in Figure 16. Photons are generated with discrete ($10\,MeV$ steps) energies from $1.6\,GeV$ up to $3.1\,GeV$. For the first two reactions shown in Figure 15, the momentum fraction can be calculated using Equn. 9. Figure 17 shows this momentum transfer t_1. The momentum transfer for the third reaction is given by Equn. 10 and is also shown in Figure 17 Finally, Figure 17 shows the center of mass energy, $\sqrt{s}$ in the KN rescattering system. This is calculated according to Equn. 11.

$$t_1 = (E_\gamma - E_{K^+})^2 - \mid (\vec{p}_\gamma \vec{p}_{K^+}) \mid^2 \quad (9)$$
$$t_2 = (E_\gamma - E_{K^+} - E_{K^-})^2 - \mid (\vec{p}_\gamma - \vec{p}_{K^+} - \vec{p}_{K^-}) \mid^2 \quad (10)$$
$$s = (E_K + m_N)^2 - \mid \vec{p}_K \mid^2 \quad (11)$$

In reaction 3, it is plausible to assume that the K^-p scatter through some resonance X^o as in Figure 15, possibly a Λ state. Similarly in reactioneq:neutron, it is plausible to assume that the K^-n scatter through some resonance X^-, possibly a Σ^- state. The rescattering of the K^- off the spectator neutron would make it impossible to see such a state in the relevant K^-N invariant mass. However, it would still be visible in the $\gamma N \rightarrow NK^+(X)$ missing mass. It would also still be directly visible in the case where the K^+ rescatters off the spectator nucleon.

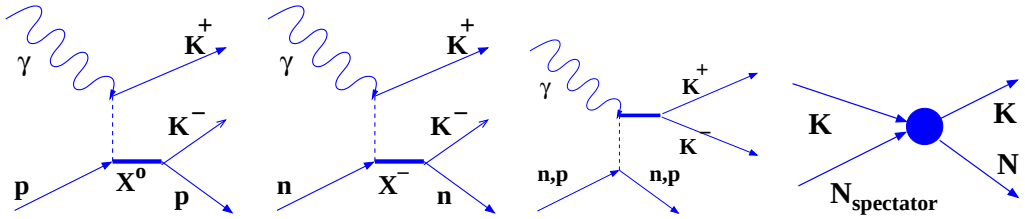

Figure 15: Photoproduction reactions off the proton and the neutron in deuterium. One of the kaons will subsequently scatter off the spectator neutron or proton.

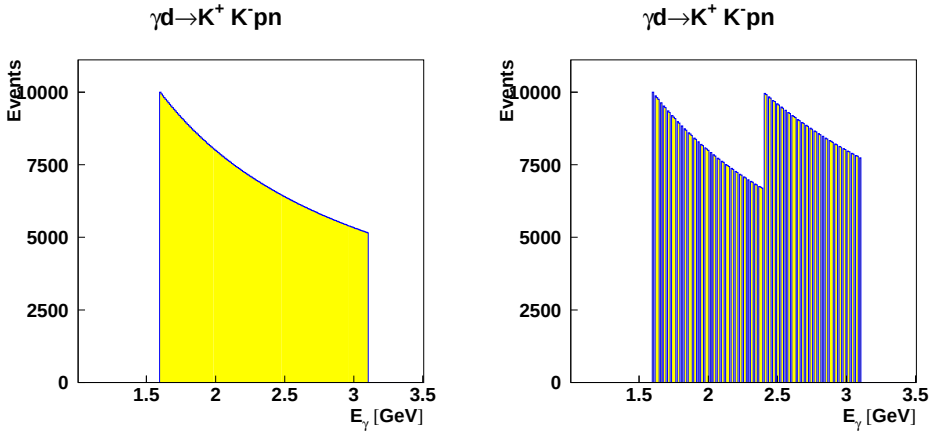

Figure 16: Number of events generated per photon energy. Studies have been made with both Energy spectrum shown. The sharp edge in the right hand spectrum seems unable to feed into the K^+n invariant mass.

Such a resonance can be simply parametrized using a non-relativistic Breit-Wigner form to weight the events, (Equn. 12). The quantity m_0 is the mass of the resonance, Γ is its width, and m is the variable mass of the K^-N system. The actual formula has been normalized such that the weight when $m = m_0$ is equal to one.

$$\mathcal{BW}(m, m_0, \Gamma) \quad = \quad \frac{m_0\Gamma}{(m - m_0)^2 + \frac{1}{4}\Gamma^2}. \tag{12}$$

We have taken three possible Λ states from the PDG [7] whose properties are given in Table 1. In the case of reaction 4, the K^-n system can scatter through a Σ^- resonance state. Possible candidates are also listed in Table 1. Figure 18 shows the effect of the three λ states on the K^-p invariant mass, (before the K^- has rescattered

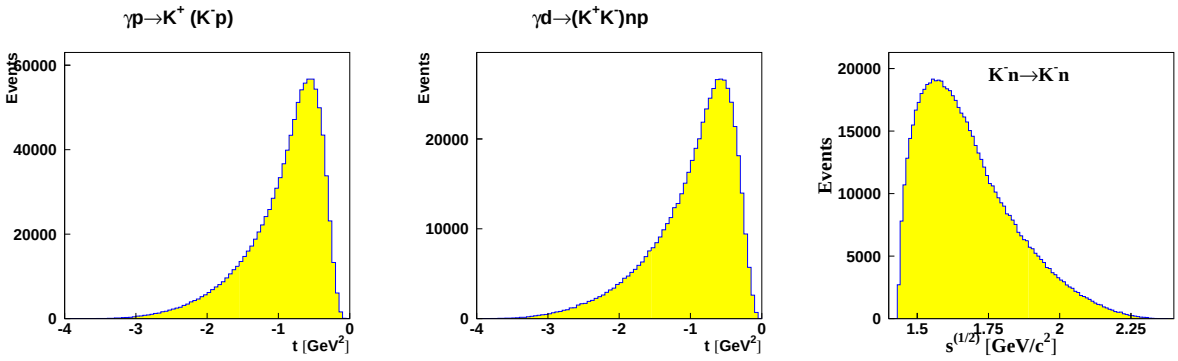

Figure 17: The left hand figure shows the momentum transfer t from the incident photon to the scattered K-nucleon system. The center figure shows the momentum transfer to the scattered nucleon off the (K^+K^-) system.The right hand figure shows the $\sqrt{s}$ of the reaction system $\gamma N \to K^+K^-N$.

off the neutron). Figure 19 shows the effect of the three Σ states on the K^-n invariant mass, (before the K^- has rescattered off the spectator proton).

Particle	Mass	Width	$(J)^P$
$\Lambda(1520)$	$1.5195\,GeV/c^2$	$0.0156\,GeV/c^2$	$(\frac{3}{2})^-$
$\Lambda(1690)$	$1.690\,GeV/c^2$	$0.060\,GeV/c^2$	$(\frac{3}{2})^-$
$\Lambda(1820)$	$1.820\,GeV/c^2$	$0.080\,GeV/c^2$	$(\frac{5}{2})^+$
$\Sigma^-(1580)$	$1.580\,GeV/c^2$	$0.015\,GeV/c^2$	$(\frac{3}{2})^-$
$\Sigma^-(1670)$	$1.670\,GeV/c^2$	$0.060\,GeV/c^2$	$(\frac{3}{2})^-$
$\Sigma^-(1775)$	$1.775\,GeV/c^2$	$0.100\,GeV/c^2$	$(\frac{5}{2})^-$
$\phi(1020)$	$1.0195\,GeV/c^2$	$0.00426\,GeV/c^2$	$(1)^-$
$f_2(1270)$	$1.270\,GeV/c^2$	$0.185\,GeV/c^2$	$(2)^{++}$
$f_2'(1525)$	$1.525\,GeV/c^2$	$0.076\,GeV/c^2$	$(2)^{++}$

Table 1: A list of the Λ, Σ and meson resonances used in this Monte Carlo study. All of these were chosen to have total spin greater than $\frac{1}{2}$ to allow for non-isotropic decay angular distributions.

It is also useful to examine the momentum distributions of the final state baryons from all of the above reactions. In the case where a Baryon is produced in the initial reaction, it has a minimum momentum of about $250\,MeV/c$, while for those events in which the baryon is rescattered into the detector, the minimum momentum goes

down to about zero. There is no minimum nor maximum momentum of a daughter baryon in the lab frame. Its spectrum depends on how fast the mother particle is moving, and the decay momentum of the state. Figure 20 shows the momentum spectrum of the final state baryons as seen in the lab frame.

There is also the related reaction where the K^+K^- is produced as a resonance, such as the $\phi(1020)$. Possible common resonances that couple to K^+K^- final states are given in table 1. These weighting applied to the K^+K^- invariant mass is shown in Figure 19.

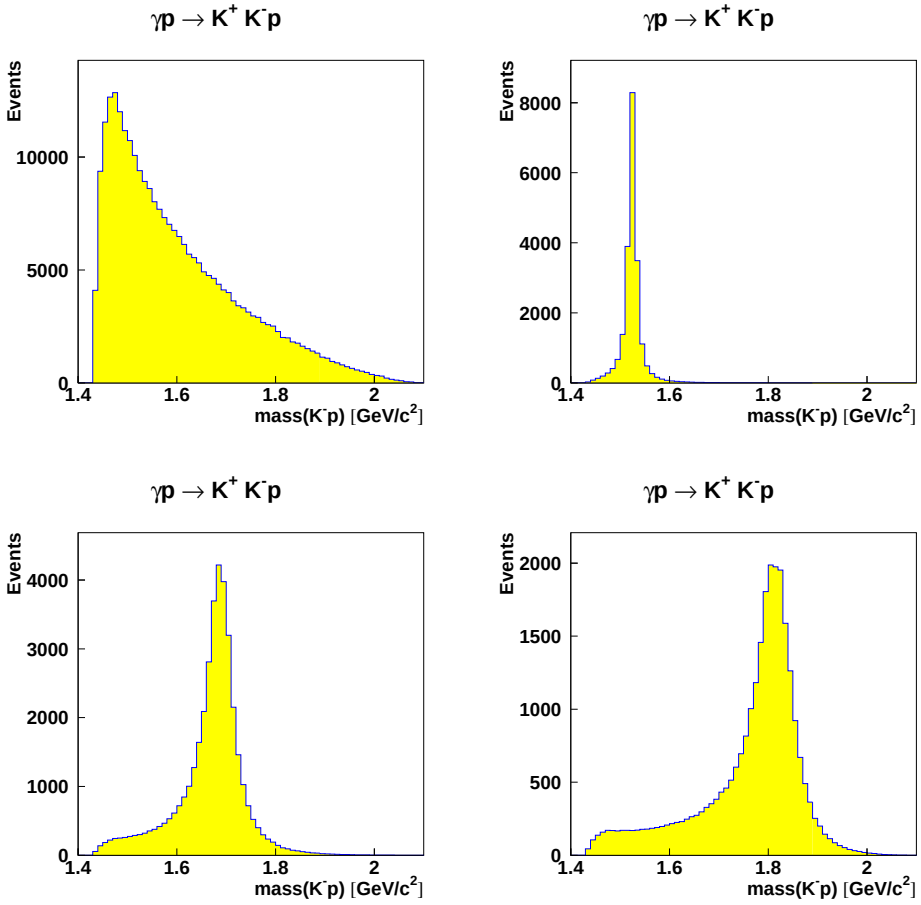

Figure 18: Different Breit Wigner weights applied to the non-rescattered K^-p system. Upper left is the unweighted distribution. Upper right is the $\Lambda(1520)$, lower left is the $\Lambda(1690)$ and lower right is the $\Lambda(1820)$.

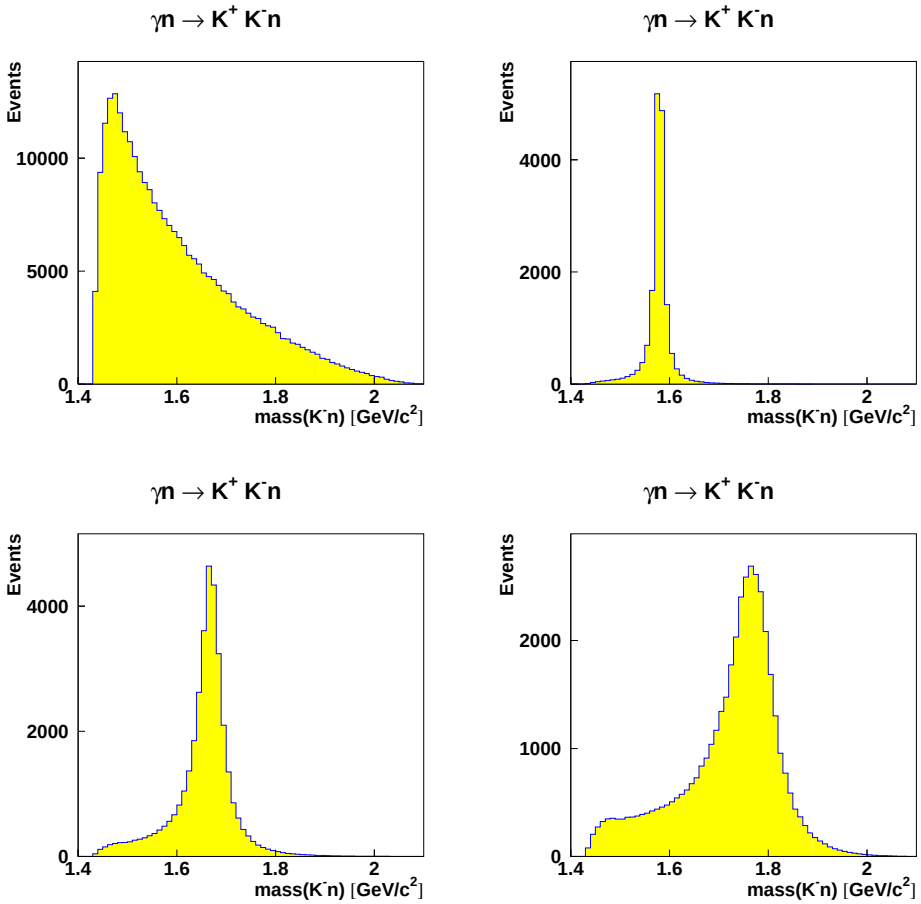

Figure 19: Different Breit Wigner weights applied to the non-rescattered K^-n system. Upper left is the unweighted distribution. Upper right is the $\Sigma^-(1580)$, lower left is the $\Sigma^-(1670)$ and lower right is the $\Sigma^-(17750)$.

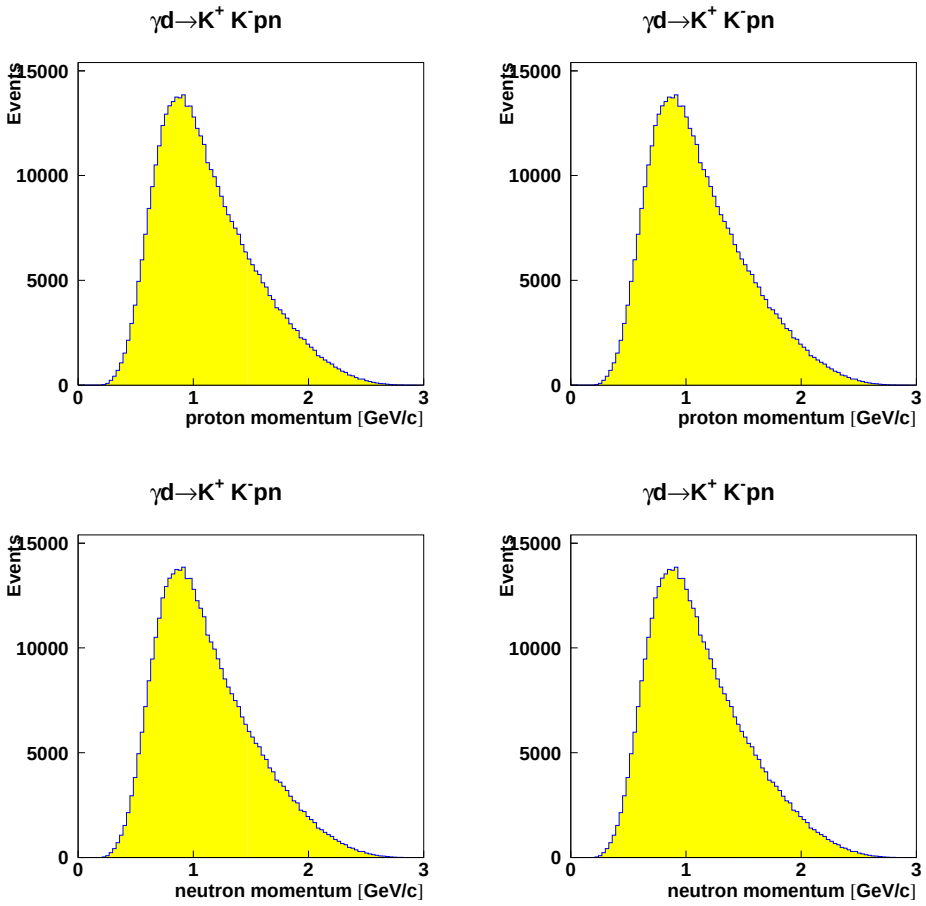

Figure 20: The final state baryon momentum as seen in the various reactions. The upper two plots are for the protons, while the lower two are for neutrons. The plots on the left are for a spectator neutron which is rescattered, while those on the right are for the spectator proton which is rescattered.

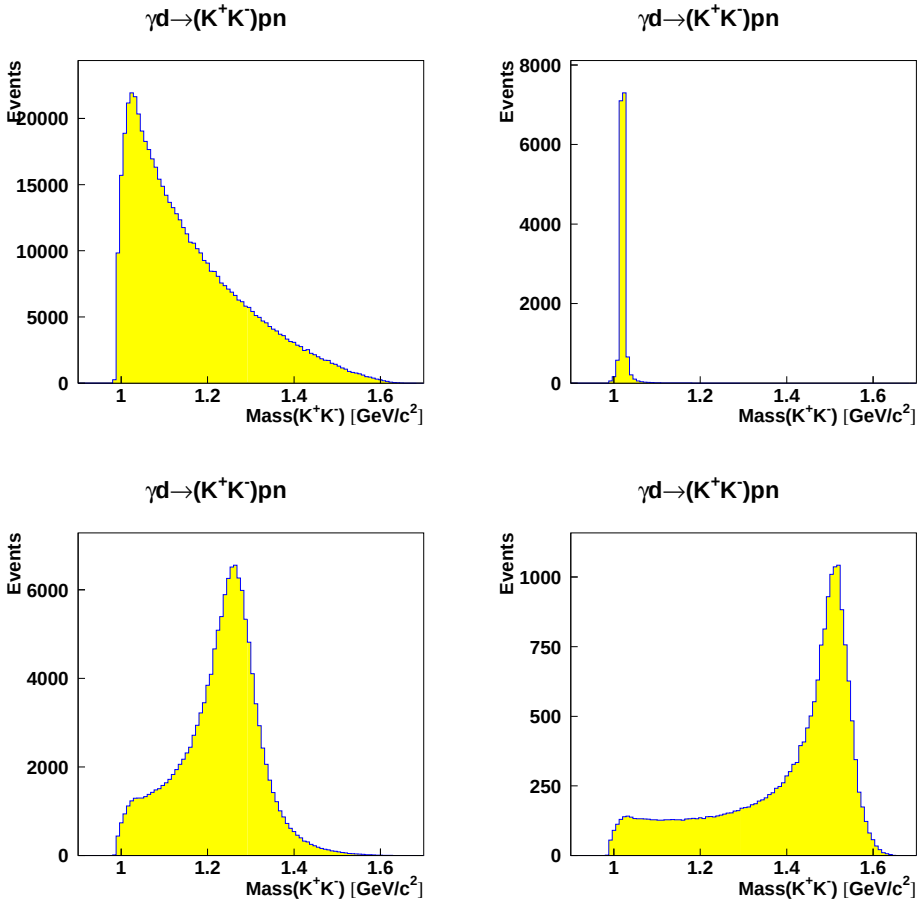

Figure 21: Different Breit Wigner weights applied to the K^+K^- system. The upper left is unweighted, the upper right is the $\phi(1020)$, the lower left is the $f_2(1270)$ and the lower right is the $f_2'(15215)$.

5 The K^+n Invariant Mass Dependencies

The K^+n invariant mass is computed as a missing mass from the process $\gamma d \rightarrow K^- pX$ as in Equn. 13.

$$m_X^2 \;=\; (E_\gamma + m_d - E_{K^-} - E_p)^2 - \mid (\vec{p}_\gamma - \vec{p}_p - \vec{p}_{K^-}) \mid^2 \qquad (13)$$

To determine if any of the other kinematic variables are correlated with m_X, we have produced scatter plots for many different quantities against the missing mass. All of these plots follow a standard layout in which the upper left figure is for reaction 3 in which the K^- rescatters off the spectator neutron, (Equn. 5. The upper right figure is for reaction 3 in which the K^+ rescatters off the spectator neutron, (Equn. 6. The lower left figure is for reaction 4 in which the K^+ rescatters off the spectator proton, (Equn. 7. Finally, the lower right figure is for reaction 4 in which the K^+ rescatters off the spectator proton, (Equn. 8.

Figure 22 shows the momentum transfer t. In all cases, restricting the data to small values of $\mid t \mid$ would enhance the low-mass K^+n system; something that would be expected from an normal $e^{-\alpha|t|}$ distribution. The data in which the K^+ rescatters is going to select a slightly higher missing mass than the case where the K^- rescatters.

Figure 23 shows the dependence on the produced K^-N system, (Λ or Σ). No strong dependences are observed, though the enhancement in the lower left hand corner of all plots could be selected by having a narrow baryon resonance at a mass of about $1.5\,GeV/c^2$.

Figure 24 shows the dependence on the cosine of the decay angle of the K^-N system as seen in its rest frame. The angle is measured between the direction of the system and the resulting K^-. There is some correlation in the lower right hand figure where forward going K^- will slightly favor lower masses.

Figure 25 shows s in the KN rescattering system plotted against the missing mass. The strong correlation in the upper right hand figure is due the fact that K^+n system is the rescatterd system. In all other cases, the is a somewhat weak correlation.

Figure 26 shows the dependence on the cosine of the rescattering angle of the kaon and the spectator nucleon as measured in their rest frame. The angle is between the direction of the KN system and the scattered kaon. A weak dependence is seen in the lower right hand figure for reaction 4 and 8.

Figure 27 shows the dependence on the final state proton momentum. In the case of reaction 4, a minimum proton momentum cut is likely to distort the missing mass spectrum.

Figure 28 shows the dependence on the final state neutron momentum. In reaction 3, a minimum neutron momentum cut is likely to distort the missing mass. The

strong correlation in the case of the upper right figure is related to the fact that the K^+n rescattering is producing the K^+n system.

Figure 29 shows the dependence on the final state K^+ momentum. No strong correlations are observed.

Figure 30 shows the dependence on the final state K^+ momentum. Strong correlations are observed in the case of reaction 3 where requiring that the proton momentum be below some value like $1\,GeV/c$ is likely to enhance the low mass K^+n mass. There is also some weak dependence observed in the lower left figure.

Figure 31 shows the dependence on the final state proton lab angle. The most likely scenario is is that the proton angle is larger than some value. While there are correlations here, it is not clear what this will do to the missing mass distribution.

Figure 32 shows the dependence on the final state K^- lab angle. Here, a minimum acceptance angle is going to have some impact on the two cases where the K^+ has resacttered off the spectator nucleon.

Figure 33 shows the dependence on the final state K^+ lab angle. In this case, a minimum angle cut is likely to have the biggest distortion on the events from reaction 4.

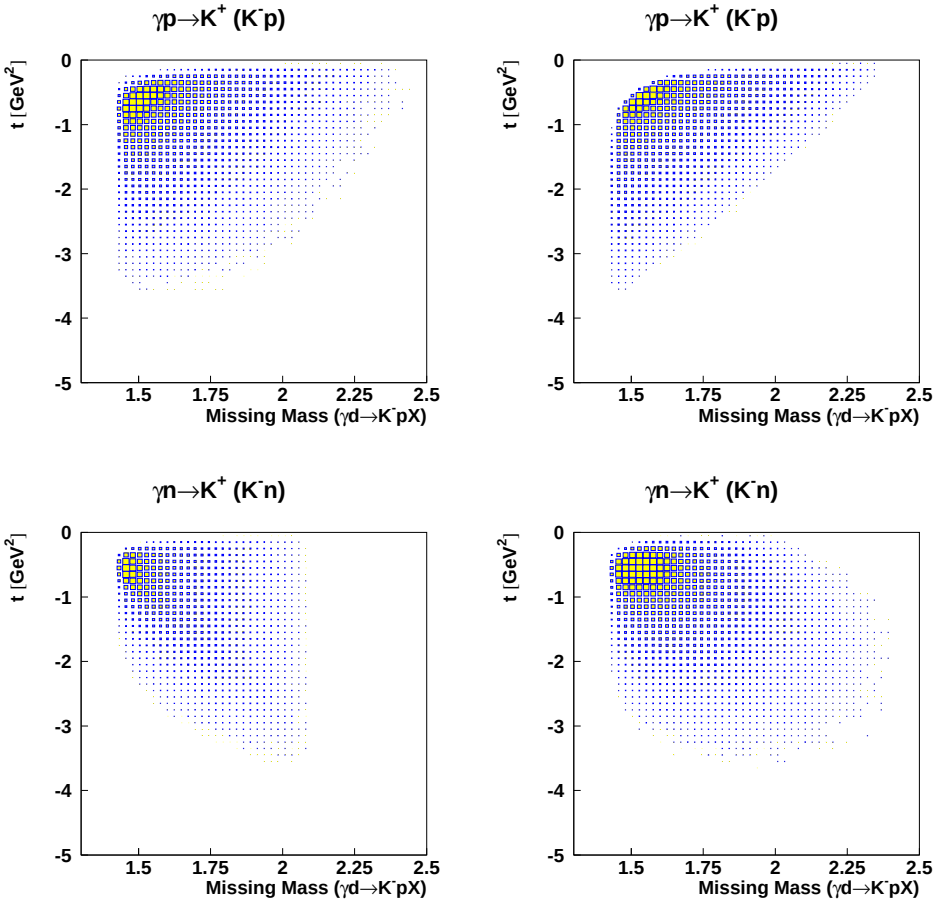

Figure 22: The momentum transfer from the photon to the scattered nucleon-K^- system plotted against the final state K^+n invariant mass, (as computed through a missing mass), $\gamma N \to K^+(K^-N)$, The upper left hand figure is for the K^-p system with the K^- rescattering off the spectator neutron. The upper right hand figure is for the K^-p system with the K^+ rescattering off the spectator neutron. The lower left hand figure is for the K^-n system with the K^- rescattering off the spectator proton. The lower right hand figure is for the K^-n system with the K^+ rescattering off the spectator proton.

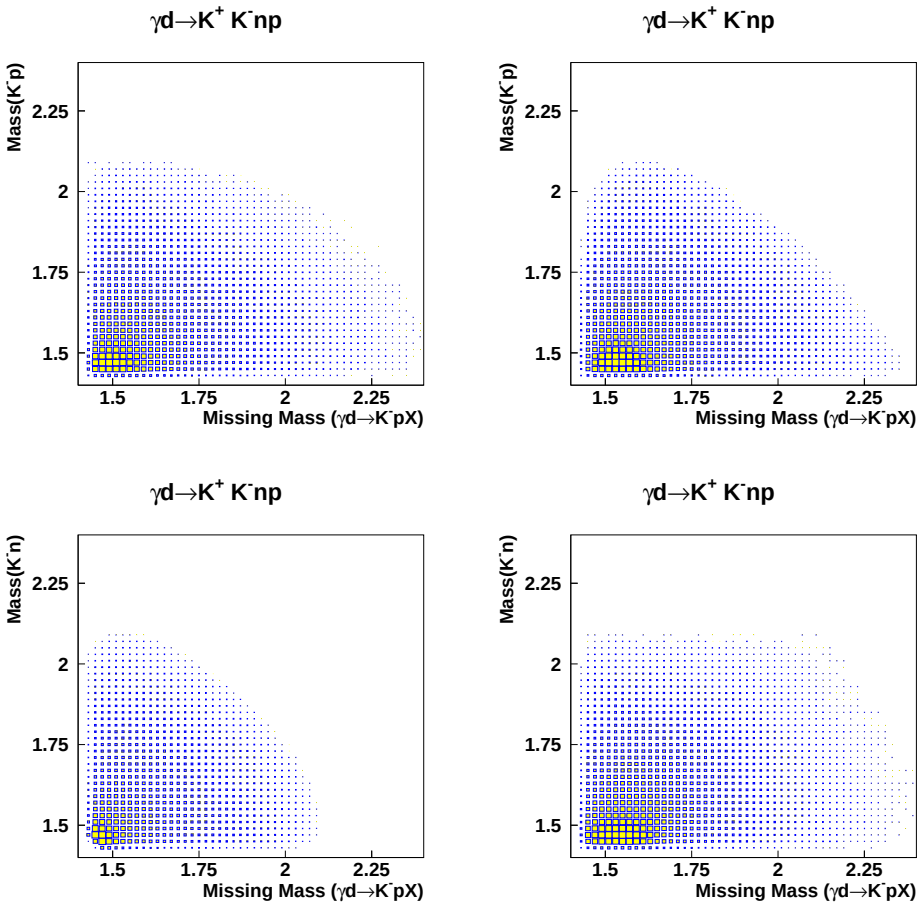

Figure 23: The mass of the produced K^-N system plotted against the final state K^+n invariant mass, (as computed through a missing mass). The upper left hand figure is for the K^-p system with the K^- rescattering off the spectator neutron. The upper right hand figure is for the K^-p system with the K^+ rescattering off the spectator neutron. The lower left hand figure is for the K^-n system with the K^- rescattering off the spectator proton. The lower right hand figure is for the K^-n system with the K^+ rescattering off the spectator proton.

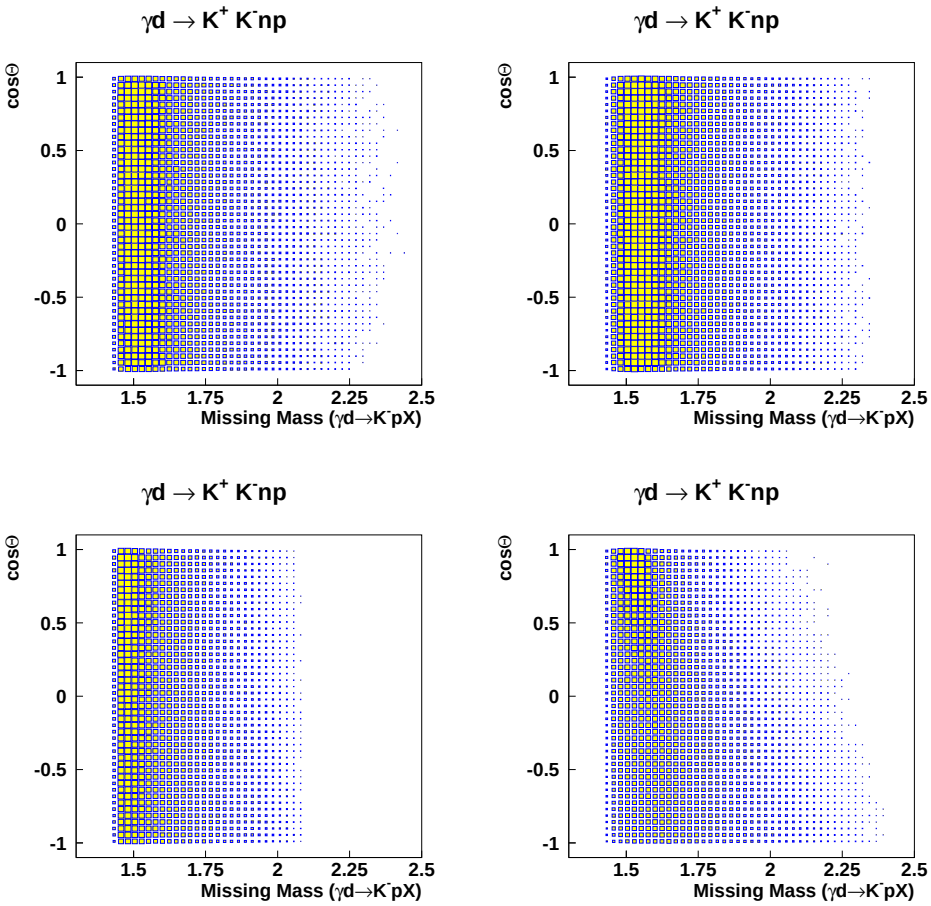

Figure 24: The decay angle ($\cos\theta$) of the KN system produced in the primary scattering plotted against K^+n invariant mass, (computed as a missing mass). Upper left is for the K^-p where the K^- rescatters off the spectator neutron. Upper right is for the K^-p where the K^+ rescatters off the spectator neutron. Lower left is for the K^-n where the K^- rescatters off the spectator proton. Lower right is for the K^-n where the K^+ rescatters off the spectator proton.

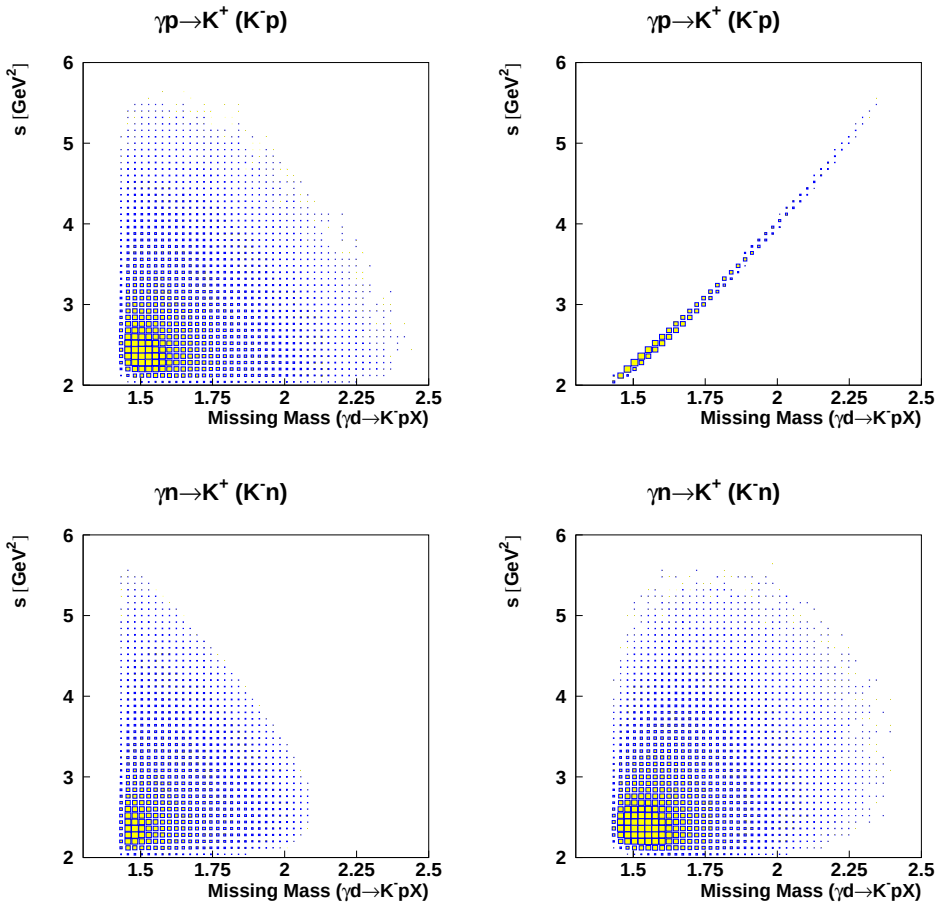

Figure 25: The center of mass energy squared, s plotted against the final state K^+n invariant mass, (as computed through a missing mass). The upper left hand figure is for the K^-p system with the K^- rescattering off the spectator neutron. The upper right hand figure is for the K^-p system with the K^+ rescattering off the spectator neutron. The lower left hand figure is for the K^-n system with the K^- rescattering off the spectator proton. The lower right hand figure is for the K^-n system with the K^+ rescattering off the spectator proton.

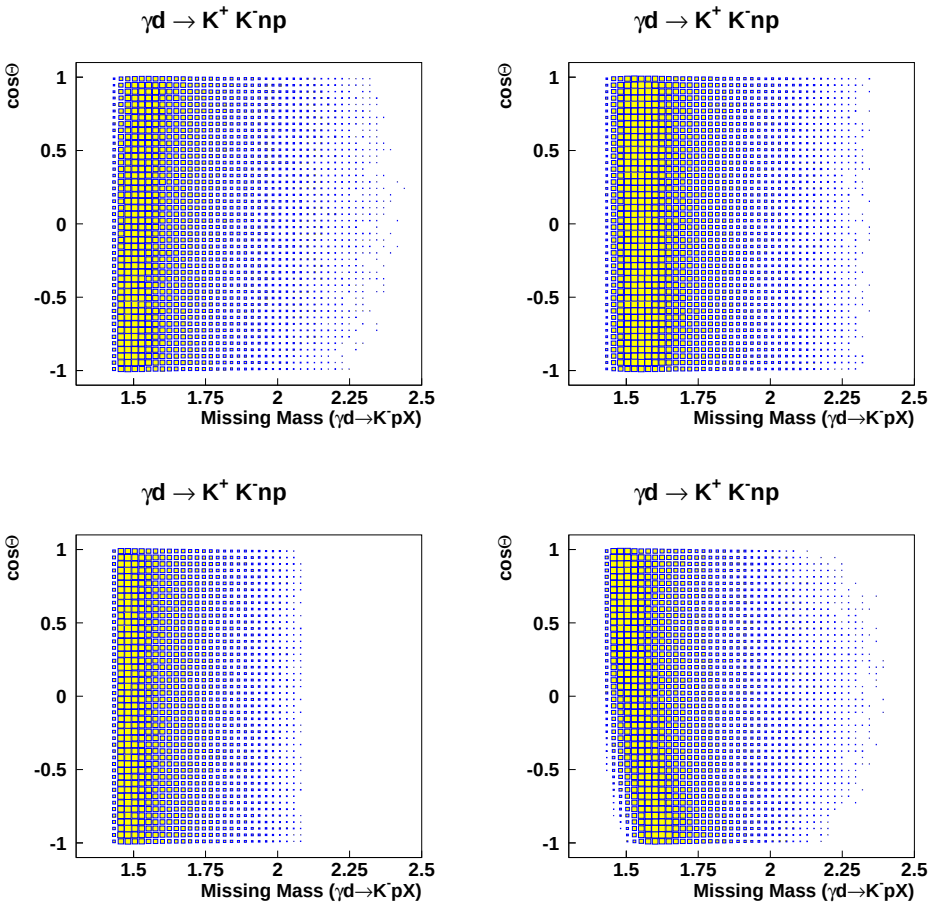

Figure 26: The scattering angle ($\cos\theta$) of the KN rescattering plotted against the K^+n invariant mass, (calculated as a missing mass). The upper left is for the K^- rescattering off the spectator neutron. Upper right is for the K^+ rescattering off the spectator neutron. Lower left is for the K^- rescattering off the spectator proton. Lower right is for the K^+ rescattering off the spectator proton.

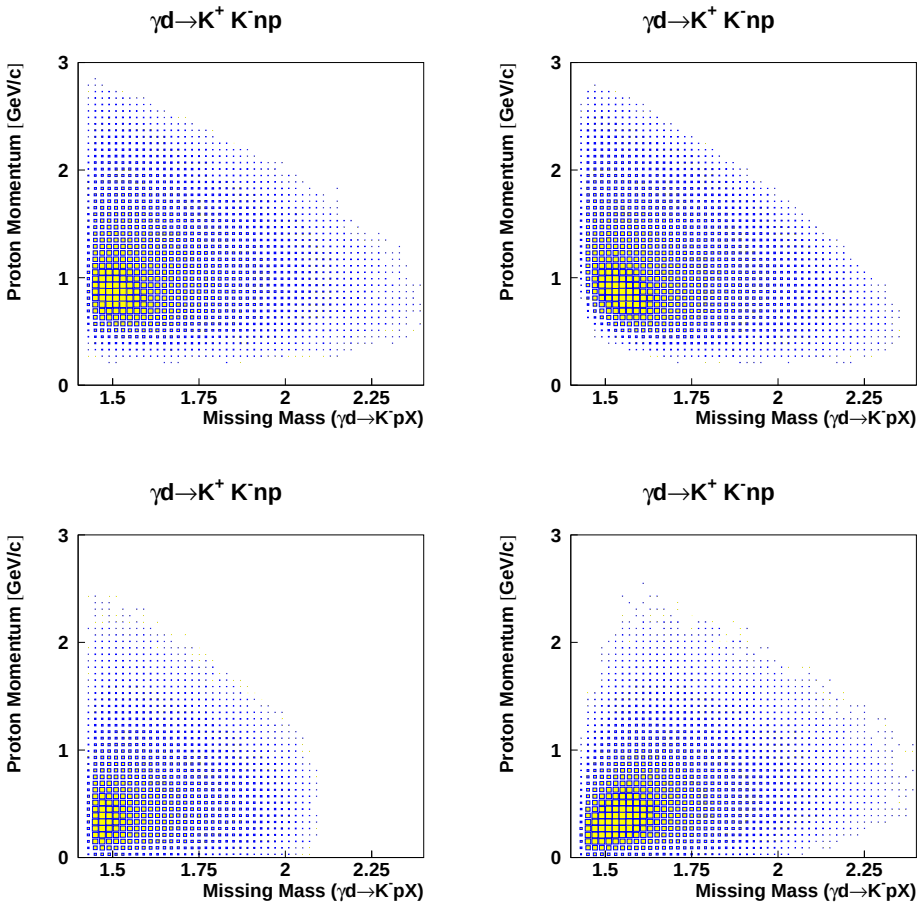

Figure 27: The momentum of the final state proton plotted against the final state K^+n invariant mass, (as computed through a missing mass). The upper left hand figure is for the K^-p system with the K^- rescattering off the spectator neutron. The upper right hand figure is for the K^-p system with the K^+ rescattering off the spectator neutron. The lower left hand figure is for the K^-n system with the K^- rescattering off the spectator proton. The lower right hand figure is for the K^-n system with the K^+ rescattering off the spectator proton.

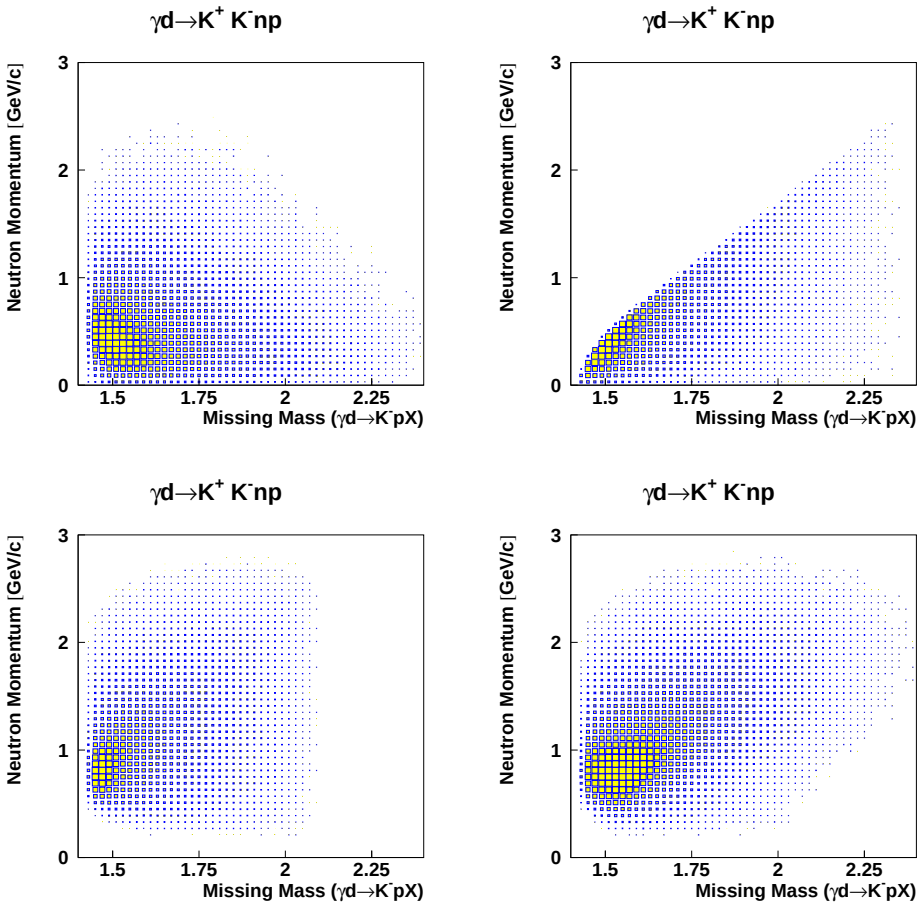

Figure 28: The momentum of the final state neutron plotted against the final state K^+n invariant mass, (as computed through a missing mass). The upper left hand figure is for the K^-p system with the K^- rescattering off the spectator neutron. The upper right hand figure is for the K^-p system with the K^+ rescattering off the spectator neutron. The lower left hand figure is for the K^-n system with the K^- rescattering off the spectator proton. The lower right hand figure is for the K^-n system with the K^+ rescattering off the spectator proton.

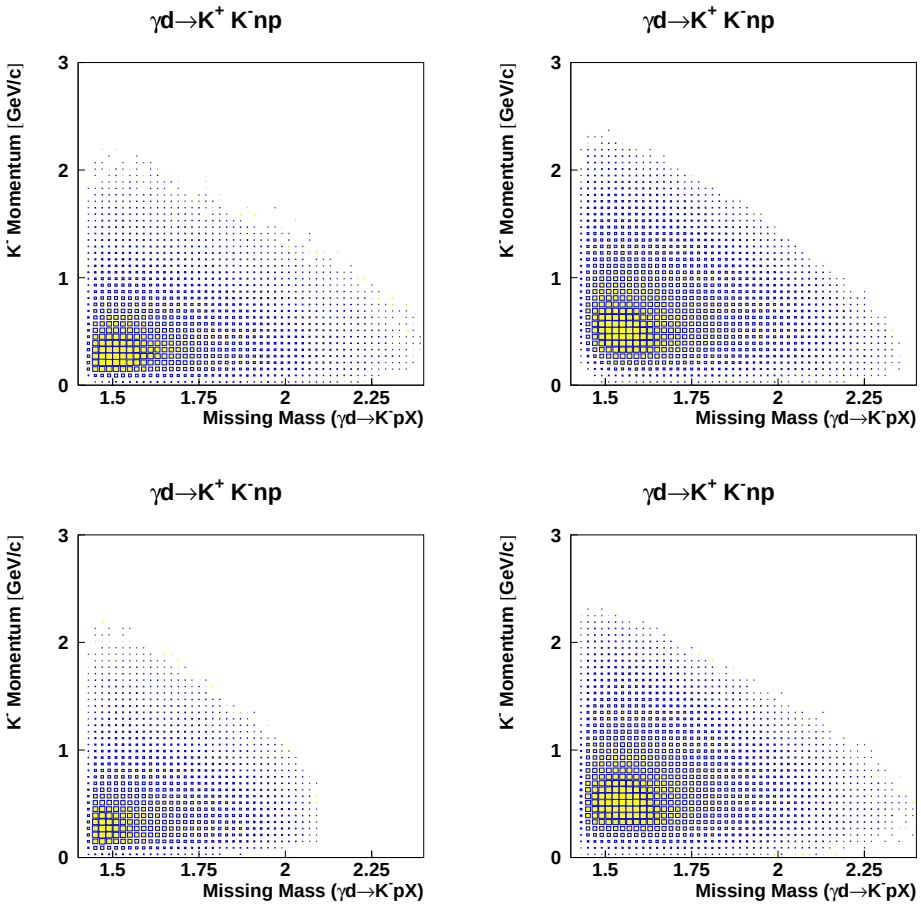

Figure 29: The momentum of the final state K^- plotted against the final state K^+n invariant mass, (as computed through a missing mass). The upper left hand figure is for the K^-p system with the K^- rescattering off the spectator neutron. The upper right hand figure is for the K^-p system with the K^+ rescattering off the spectator neutron. The lower left hand figure is for the K^-n system with the K^- rescattering off the spectator proton. The lower right hand figure is for the K^-n system with the K^+ rescattering off the spectator proton.

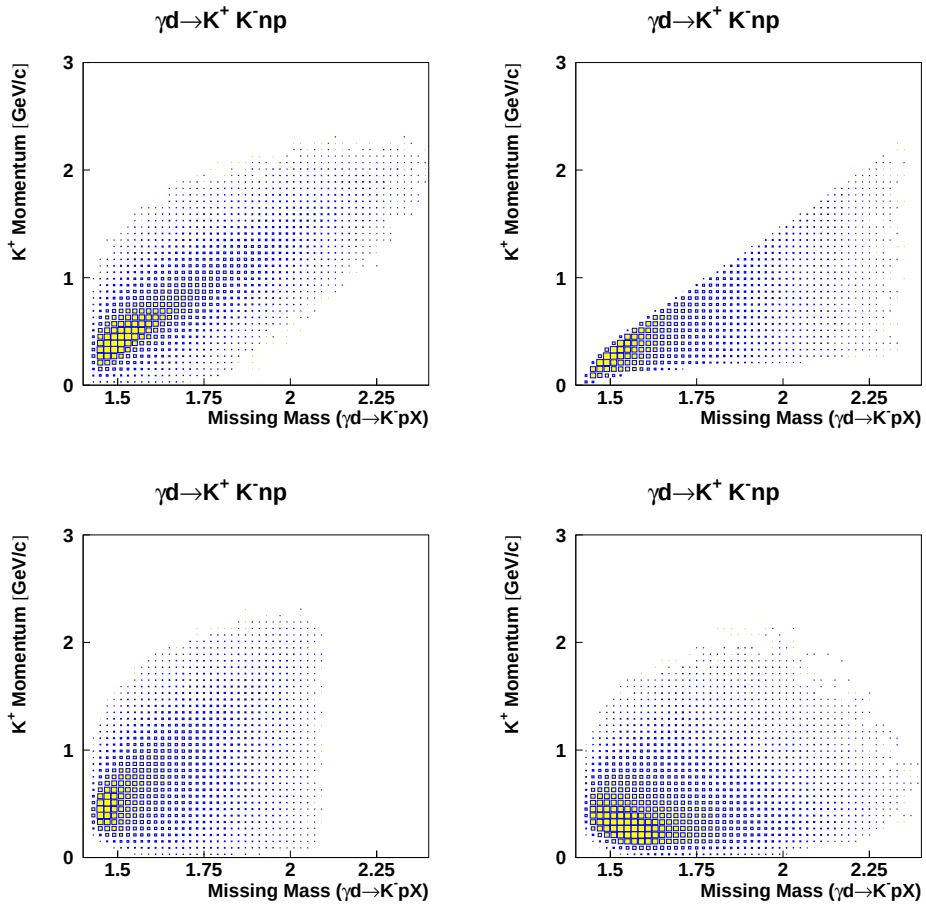

Figure 30: The momentum of the final state K^+ plotted against the final state K^+n invariant mass, (as computed through a missing mass). The upper left hand figure is for the K^-p system with the K^- rescattering off the spectator neutron. The upper right hand figure is for the K^-p system with the K^+ rescattering off the spectator neutron. The lower left hand figure is for the K^-n system with the K^- rescattering off the spectator proton. The lower right hand figure is for the K^-n system with the K^+ rescattering off the spectator proton.

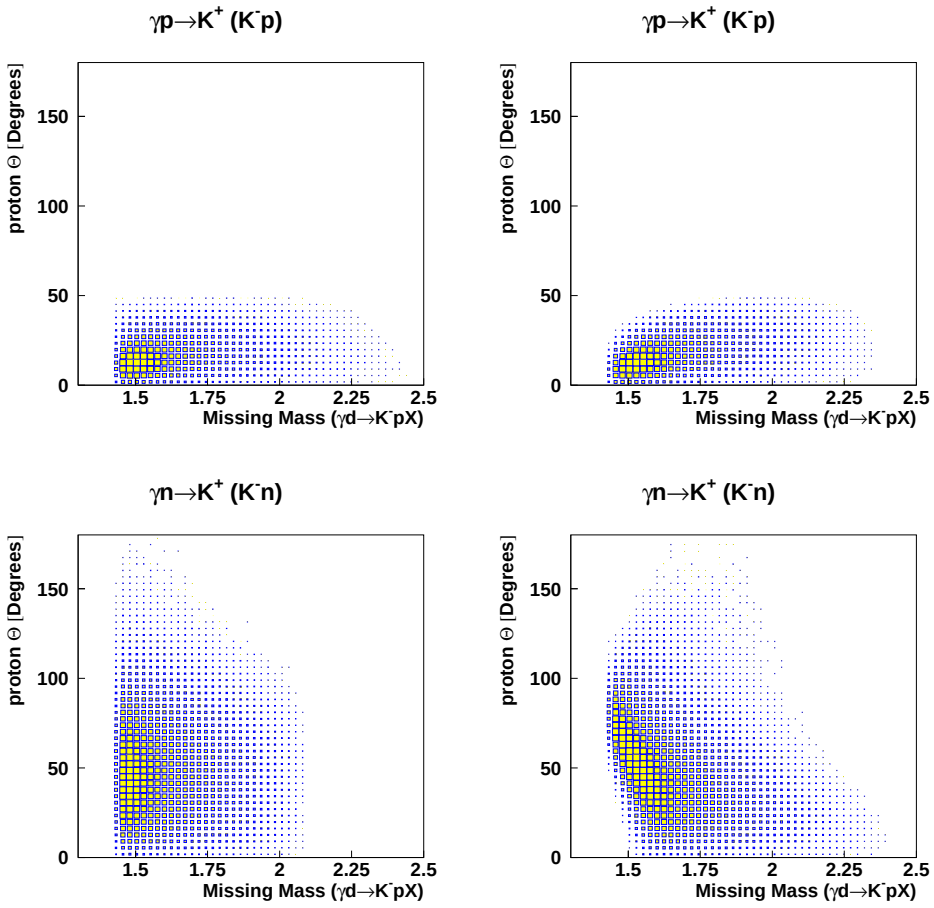

Figure 31: The measured angle of the final state proton (in the lab) plotted against the K^+n invariant mass, (calculated as a missing mass). The upper left plot is for the K^- rescattering off the spectator neutron. Upper right is for the K^+ rescattering off the spectator neutron. Lower left is for the K^- rescattering off the spectator proton. Lower right is for the K^+ rescattering off the spectator proton.

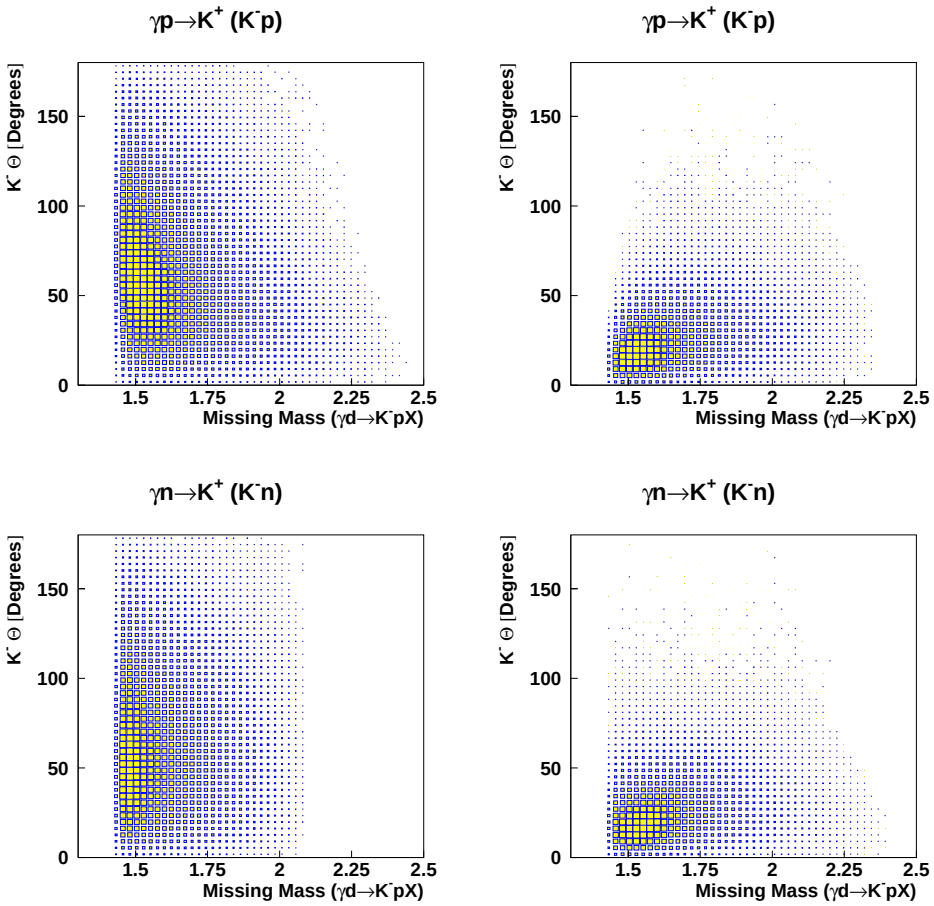

Figure 32: The measured angle of the final state K^- (in the lab) plotted against the K^+n invariant mass, (calculated as a missing mass). The upper left plot is for the K^- rescattering off the spectator neutron. Upper right is for the K^+ rescattering off the spectator neutron. Lower left is for the K^- rescattering off the spectator proton. Lower right is for the K^+ rescattering off the spectator proton.

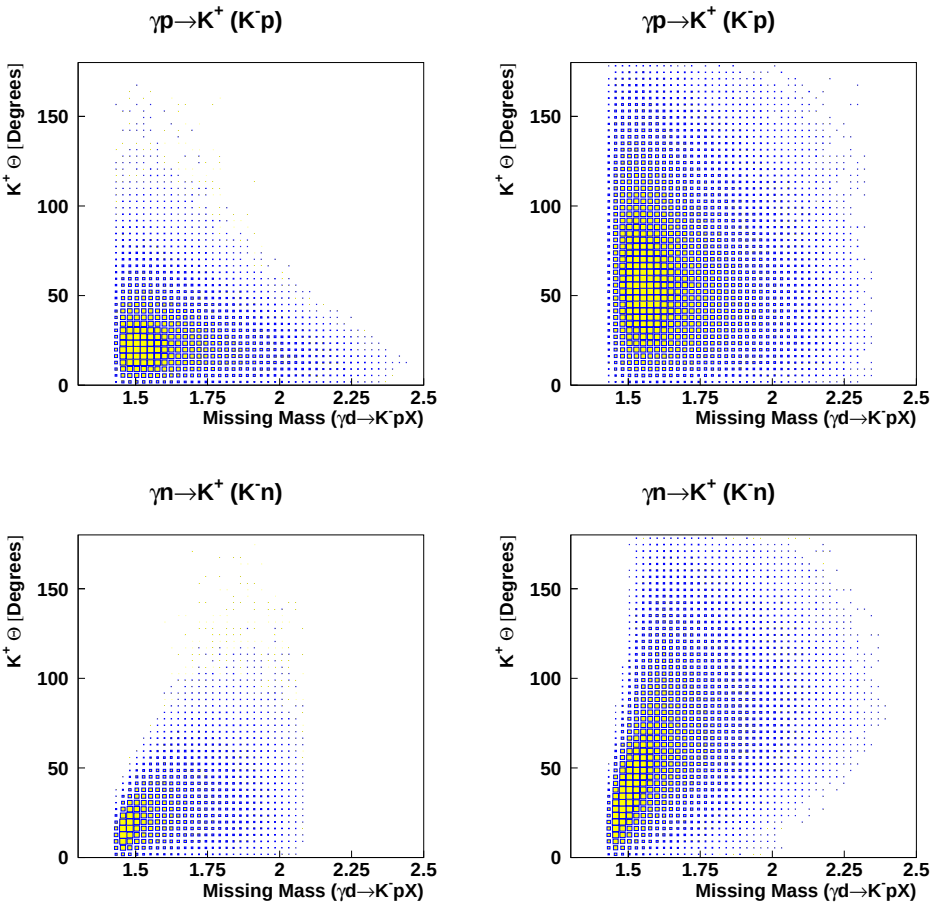

Figure 33: The measured angle of the final state K^+ (in the lab) plotted against the K^+n invariant mass, (calculated as a missing mass). The upper left plot is for the K^- rescattering off the spectator neutron. Upper right is for the K^+ rescattering off the spectator neutron. Lower left is for the K^- rescattering off the spectator proton. Lower right is for the K^+ rescattering off the spectator proton.

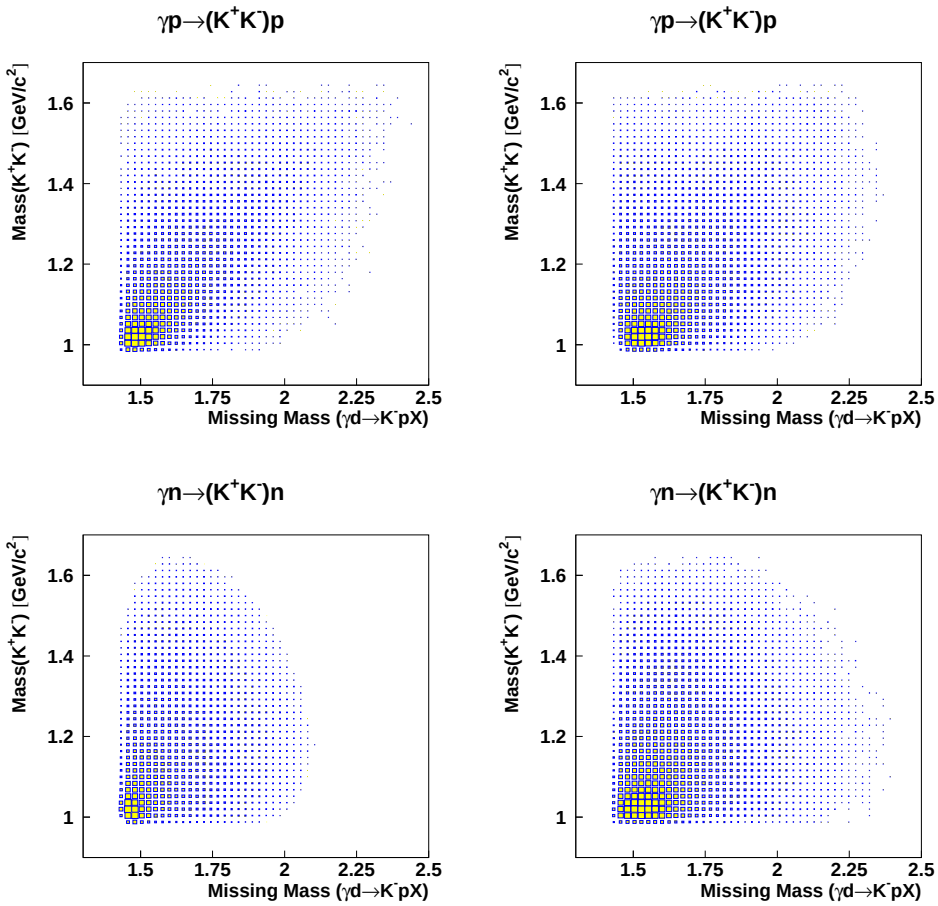

Figure 34: The mass of the K^+K^- system plotted against the final state K^+n invariant mass, (as computed through a missing mass), $\gamma N \to (K^+K^-)N$. The upper left hand figure is for the K^-p system with the K^- rescattering off the spectator neutron. The upper right hand figure is for the K^-p system with the K^+ rescattering off the spectator neutron. The lower left hand figure is for the K^-n system with the K^- rescattering off the spectator proton. The lower right hand figure is for the K^-n system with the K^+ rescattering off the spectator proton.

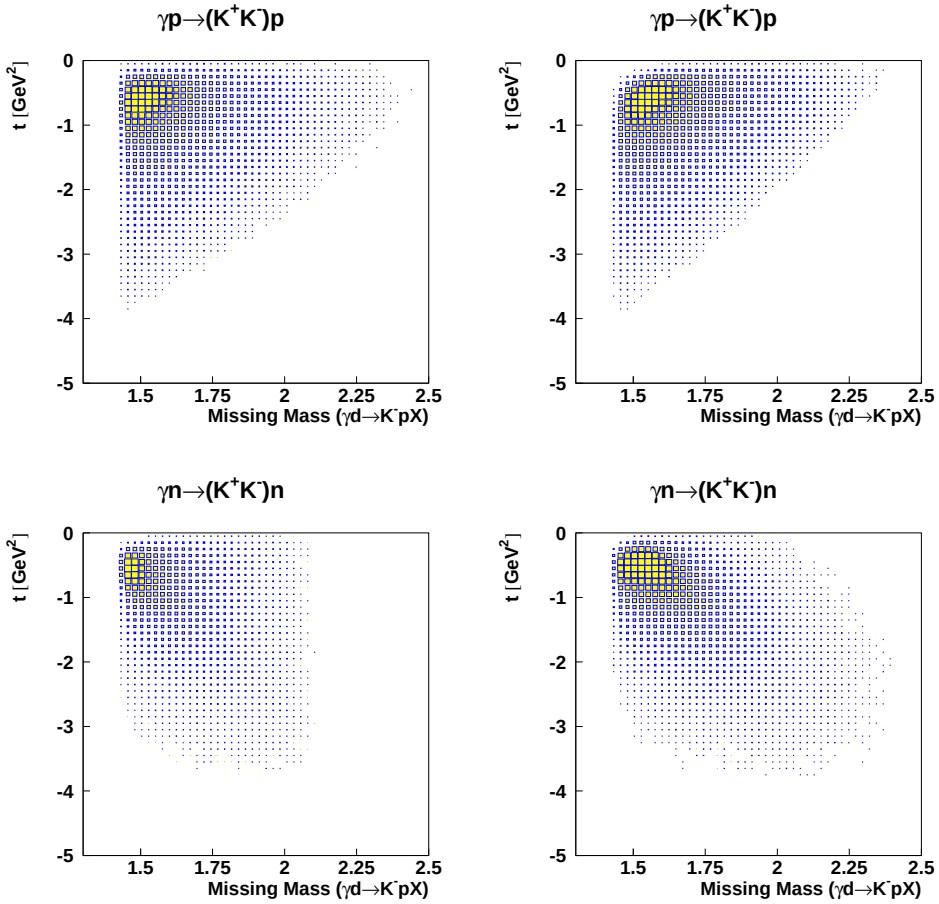

Figure 35: The momentum transfer from the photon to the scattered nucleon plotted against the final state K^+n invariant mass, (as computed through a missing mass), $\gamma N \rightarrow K^+K^-)N$. The upper left hand figure is for the K^-p system with the K^- rescattering off the spectator neutron. The upper right hand figure is for the K^-p system with the K^+ rescattering off the spectator neutron. The lower left hand figure is for the K^-n system with the K^- rescattering off the spectator proton. The lower right hand figure is for the K^-n system with the K^+ rescattering off the spectator proton.

6 Kaon Decay

In addition to the raw correlations discussed in the previous section, an additional physics consideration is the decay of kaons in the detector. Kaons have a finite

lifetime, ($12.4\,ns$ [7]). We can compute the time that it takes a particle to travel $1\,m$ in the detector as

$$t = (1m)/\beta c = (0.333\,ns)/\beta$$

These time-of-flights are shown in Figure 36 for all K^+ in the data sample, for both the rescattered K^- and the rescattered K^+. Figure 37 shows the same plots for the K^-. If we assume that K's which decay before 3m are lost due to incorrect reconstruction of the event, then the probability of loosing an event is given as $P = \exp(-3 \times t/\tau_K)$ where the lifetime of the kaon, $\tau_K = 12.4\,ns$. Figure 38 shows the momentum distribution for K^+ both before and after this decay cut has been applied. Figure 39 shows the same for the K^-. In order to examine this structure a bit more closely, we have applied loose cuts on the reconstructed particles in the events. These are given in Table 2.

Quant.	Min.	Max.	Description
p_p	$0.3\,GeV/c$	none	proton momentum
θ_{K^-}	10°	none	K^- scattering angle

Table 2:

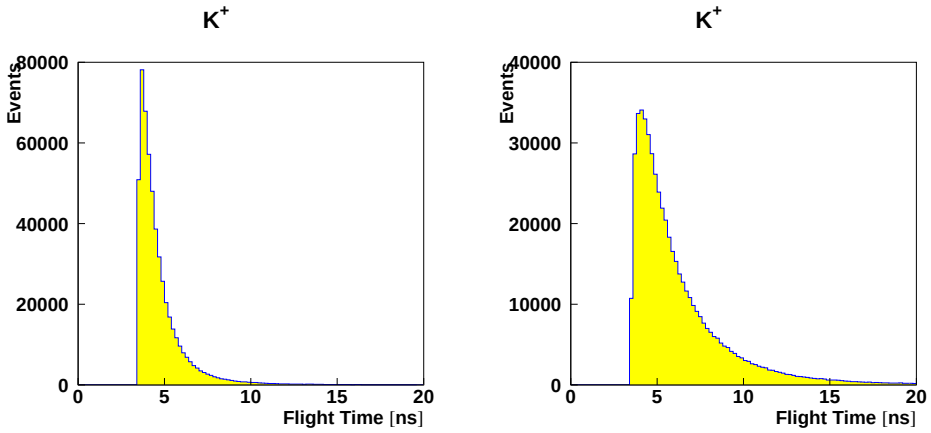

Figure 36: The time for the K^+ to travel $1\,m$ as measured in ns. The left hand figure has the K^- rescattering off the spectator nucleon, while the right hand figure has the K^+ rescattering.

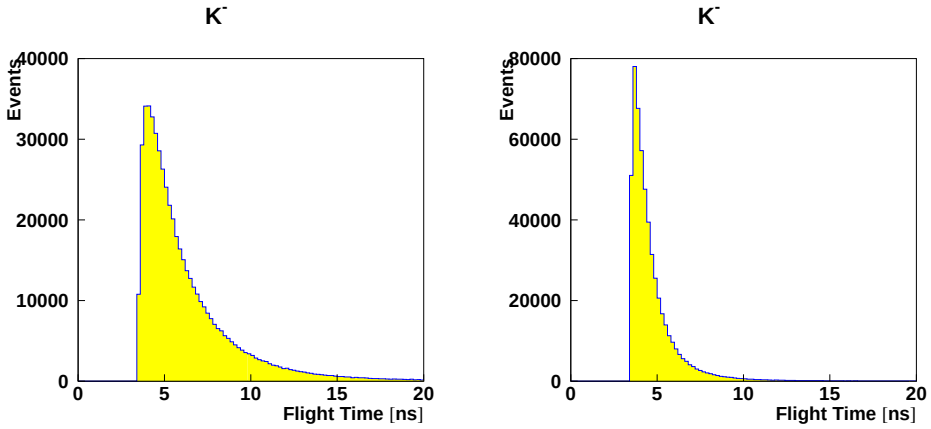

Figure 37: The time for the K^- to travel $1\,m$ as measured in ns. The left hand figure has the K^- rescattering off the spectator nucleon, while the right hand figure has the K^+ rescattering.

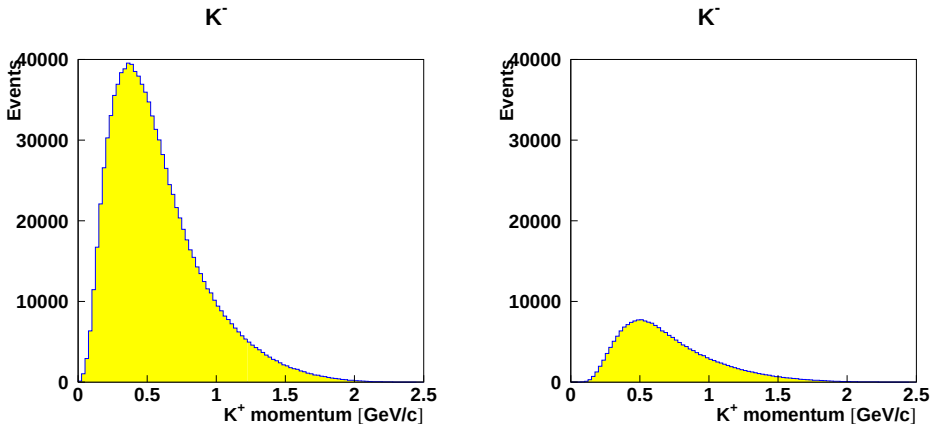

Figure 38: The momentum distributions for K^+ in all events. The plot on the left is for all events, while that on the right is for those surviving a flight path of $3\,m$ before decaying.

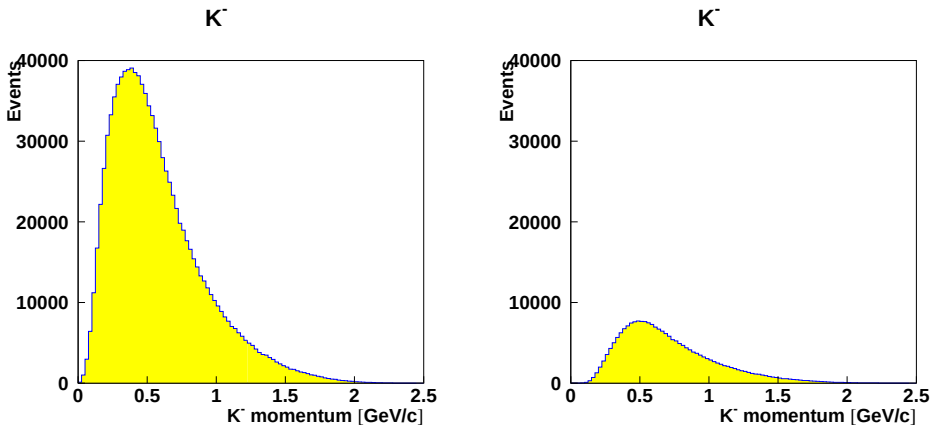

Figure 39: The momentum distributions for K^- in all events. The plot on the left is for all events, while that on the right is for those surviving a flight path of $3\,m$ before decaying.

7 Details on $\gamma d \to (K^+K^-)np$

A possible related reaction is the case where the K^+K^- system forms a resonance, and one of the daughter kaons then rescatters off the spectator nucleon in the event. The most logical choice here is the $\phi(1020)$. It is also known that such t-channel processes are produced with a t-distribution that goes like $e^{-\alpha|t|}$, with α in the range of 3 to 5.

Figure 40 shows the K^+n mass for events in which the initial K^+K^- pair originate from a $\phi(1020)$ with a slope parameter of $\alpha = 4$. The ϕ is then allowed to decay isotropically in its rest frame. Figure 41 is the same plot, except that the $\phi(1020)$ decays with a $\cos^2\theta$ distribution relative to the direction of the ϕ. Figure 42 has the additional requirement that the final state K^+K^- pair reconstruct to a mass larger that $1.06\,GeV/c^2$. What is particularly interesting in these plots is the lower right hand figure which corresponds to the reaction $\gamma n \to \phi n$, with the K^+ from the ϕs decay rescattering off the spectator proton in the event.

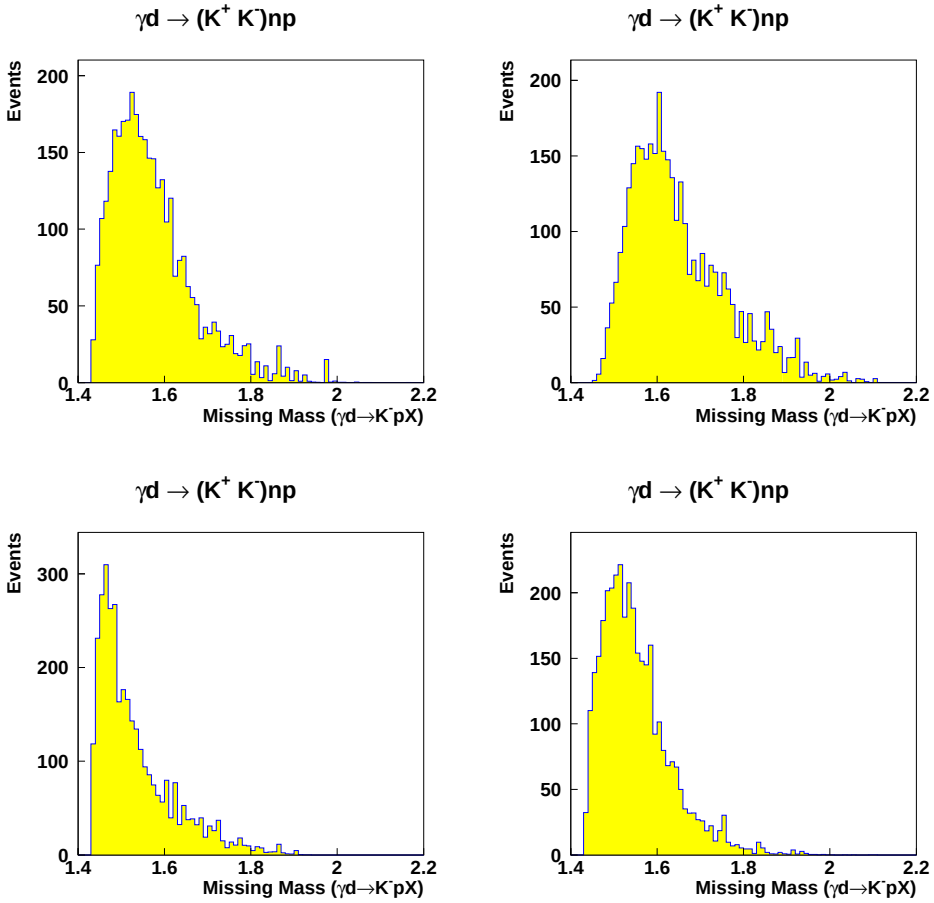

Figure 40: The missing mass for the case when the K^+K^- system originates from an isotropically decaying $\phi(1020)$ which has been produced with an $\alpha = 4$ slope parameter, and the kaons are allowed to decay. The upper left hand figure is for the K^-p system with the K^- rescattering off the spectator neutron. The upper right hand figure is for the K^-p system with the K^+ rescattering off the spectator neutron. The lower left hand figure is for the K^-n system with the K^- rescattering off the spectator proton. The lower right hand figure is for the K^-n system with the K^+ rescattering off the spectator proton.

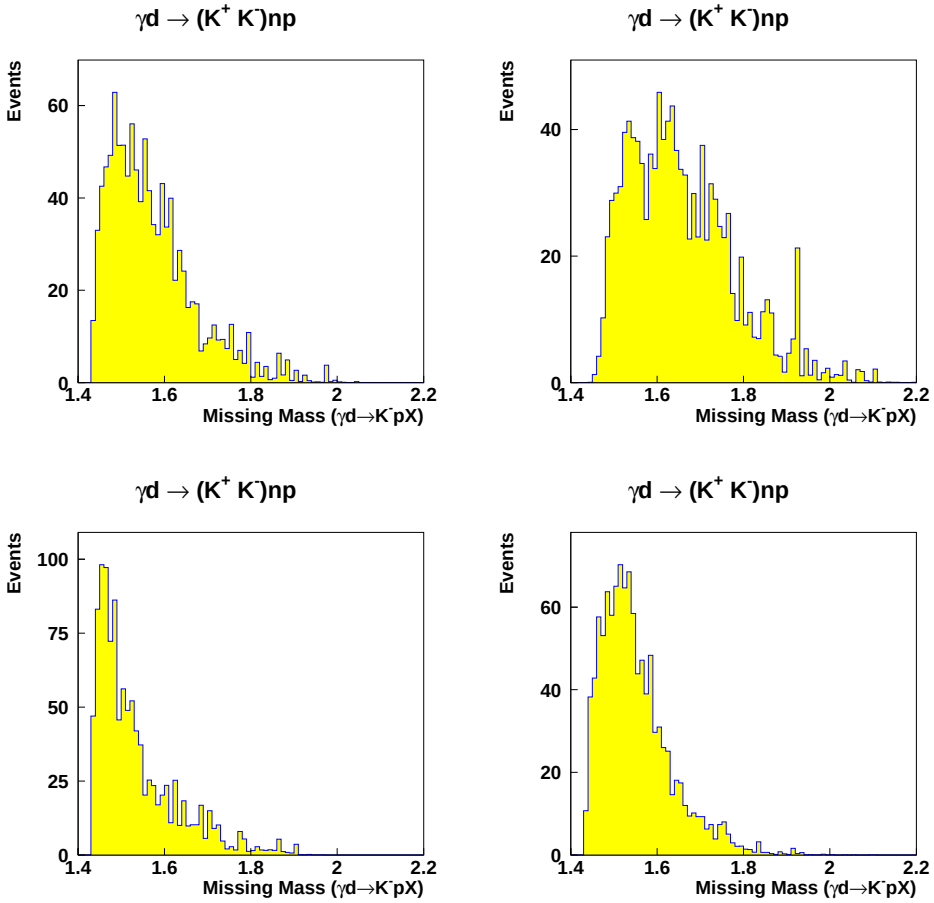

Figure 41: The missing mass for the case when the K^+K^- system originates from a $\phi(1020)$ which has been produced with an $\alpha = 4$ slope parameter. The ϕ decays according to a $\cos^2\theta$ distribution, and the kaons are allowed to decay. The upper left hand figure is for the K^-p system with the K^- rescattering off the spectator neutron. The upper right hand figure is for the K^-p system with the K^+ rescattering off the spectator neutron. The lower left hand figure is for the K^-n system with the K^- rescattering off the spectator proton. The lower right hand figure is for the K^-n system with the K^+ rescattering off the spectator proton.

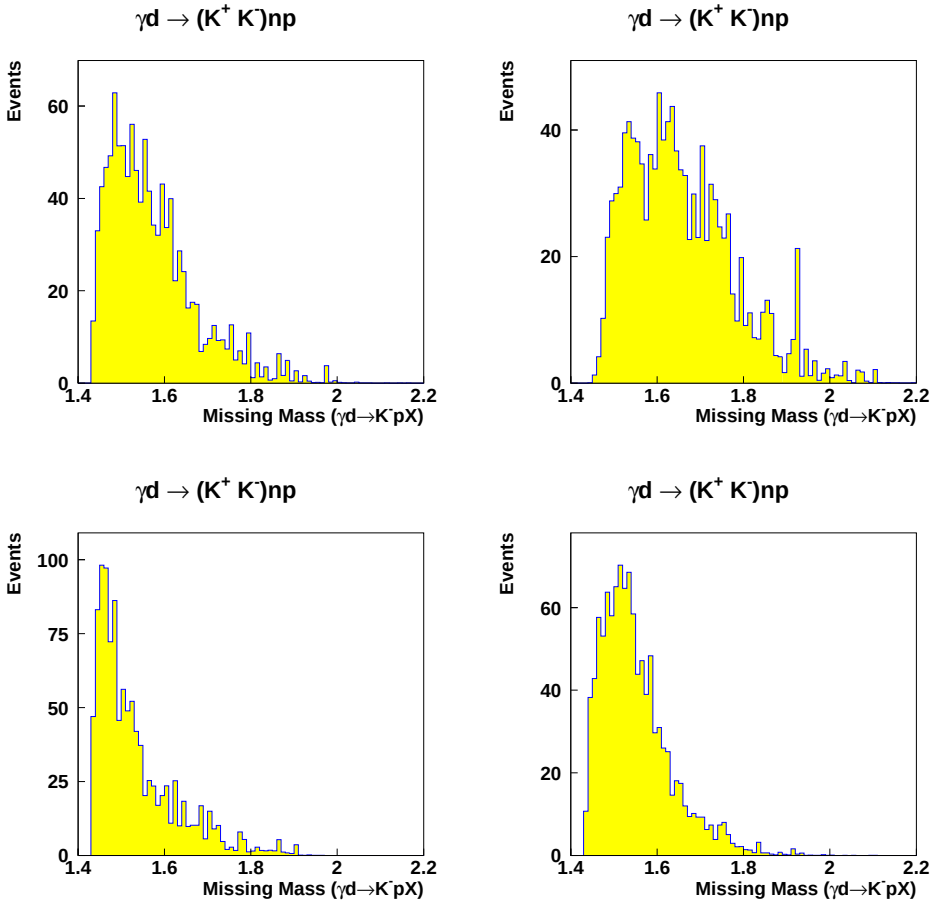

Figure 42: The missing mass for the case when the K^+K^- system originates from a $\phi(1020)$ which has been produced with an $\alpha = 4$ slope parameter. The ϕ decays according to a $\cos^2\theta$ distribution, and the kaons are allowed to decay. We have also excluded events in which the final state K^+K^- pair reconstruct to a mass less than $1.06\,GeV/c^2$. The upper left hand figure is for the K^-p system with the K^- rescattering off the spectator neutron. The upper right hand figure is for the K^-p system with the K^+ rescattering off the spectator neutron. The lower left hand figure is for the K^-n system with the K^- rescattering off the spectator proton. The lower right hand figure is for the K^-n system with the K^+ rescattering off the spectator proton.

8 Specific Cuts

The following are a series of plots of the K^+n invariant mass using different cuts, and weights applied to the K^-N systems. For the most part, the captions are self contained descriptions.

A somewhat restrictive cut is to require that the detected proton have at least $0.30\,GeV/c$ of momentum. Figure 47 shows a series of plots employing this cut in which the K^- rescatters off the spectator neutron in the event. Going left to right and top to bottom this shows the missing mass for all events in which the proton has sufficient momentum. Then the K^-p system is required to have come from a $\Lambda(1520)$ which decays isotropically in its rest frame. The next has the $\Lambda(1520)$ decaying with a $\cos^2$ distribution and the final one is for a $\sin^2$ distribution. Figure 48 repeats this for the case in which the K^+ scatters off the spectator neutron in the event.

Figure 49 shows a series of plots employing this cut in which the K^- rescatters off the spectator proton in the event. Going left to right and top to bottom this shows the missing mass for all events in which the proton has sufficient momentum. Then the K^-n system is required to have come from a $\Sigma(1580)$ which decays isotropically in its rest frame. The next has the $\Sigma(1580)$ decaying with a $\cos^2$ distribution and the final one is for a $\sin^2$ distribution. Figure 48 repeats this for the case in which the K^+ scatters off the spectator proton in the event.

Figure 43 shows this distribution for events in which the K^- rescatters off the spectator neutron for all events, and for events weighted for the three Λ resonances in the previous section. The largest effect is observed in the upper right figure where events are assumed to have come from the $\Lambda(1520)$. Here, there is a slight sharpening of the phase space peak at about $1.6\,GeV/c^2$. Figure 44 shows the same distribution for events in which the K^+ rescatters off the spectator neutron.

Figure 45 shows the invariant mass distribution for events in which the K^- rescatters off the spectator proton for all events, and for events weighted for the three Σ resonances in the previous section. Figure 46 shows the same distribution for events in which the K^+ rescatters off the spectator proton.

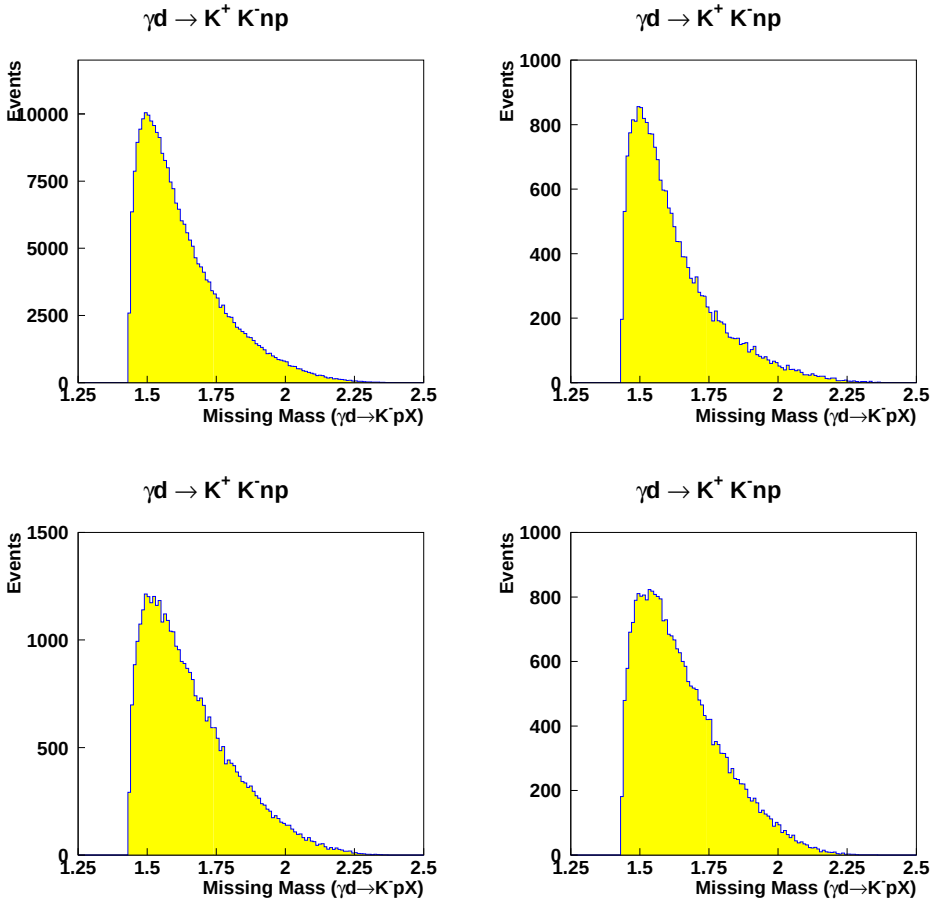

Figure 43: The K^+n invariant mass as weighted by the three different resonance in Figure 18 in the K^-p (Λ) system. The upper left is for all data, the upper right is for the $\Lambda(1520)$, the lower left is for the $\Lambda(1690)$ and the lower right is for the $\Lambda(1820)$. This reaction assumes that the K^- scatters off the spectator neutron in the reaction.

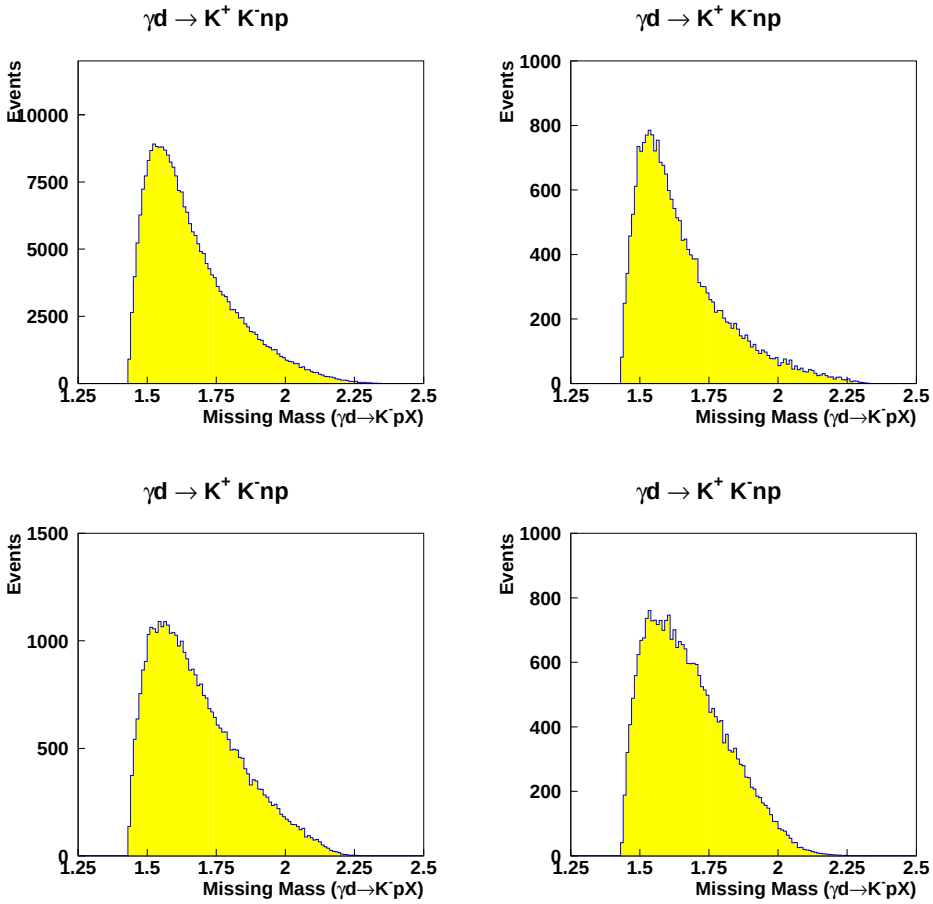

Figure 44: The K^+n invariant mass as weighted by the three different resonance in Figure 18 in the K^-p (Λ) system. The upper left is for all data, the upper right is for the $\Lambda(1520)$, the lower left is for the $\Lambda(1690)$ and the lower right is for the $\Lambda(1820)$.This reaction assumes that the K^+ scatters off the spectator neutron in the reaction.

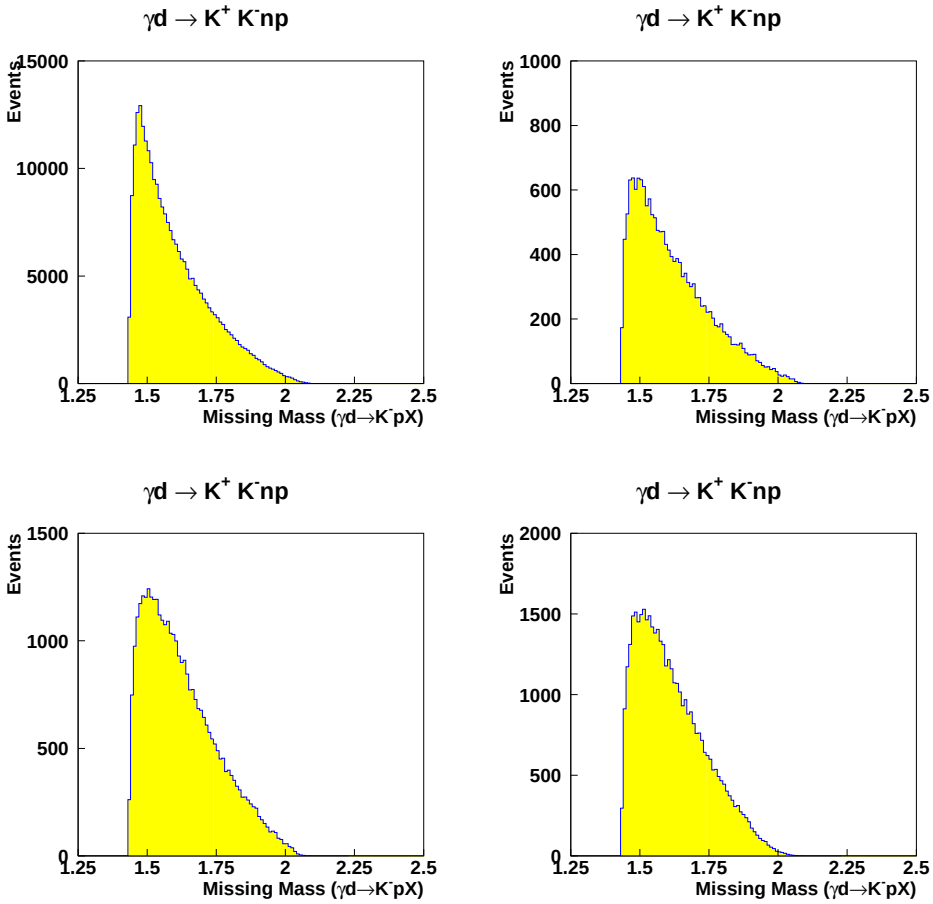

Figure 45: The K^+n invariant mass as weighted by the three different resonance in Figure 18 in the K^-n (Σ) system. The upper left is for all data, the upper right is for the $\Sigma(1580)$, the lower left is for the $\Sigma(1670)$ and the lower right is for the $\Sigma(1775)$.This reaction assumes that the K^- scatters off the spectator proton in the reaction.

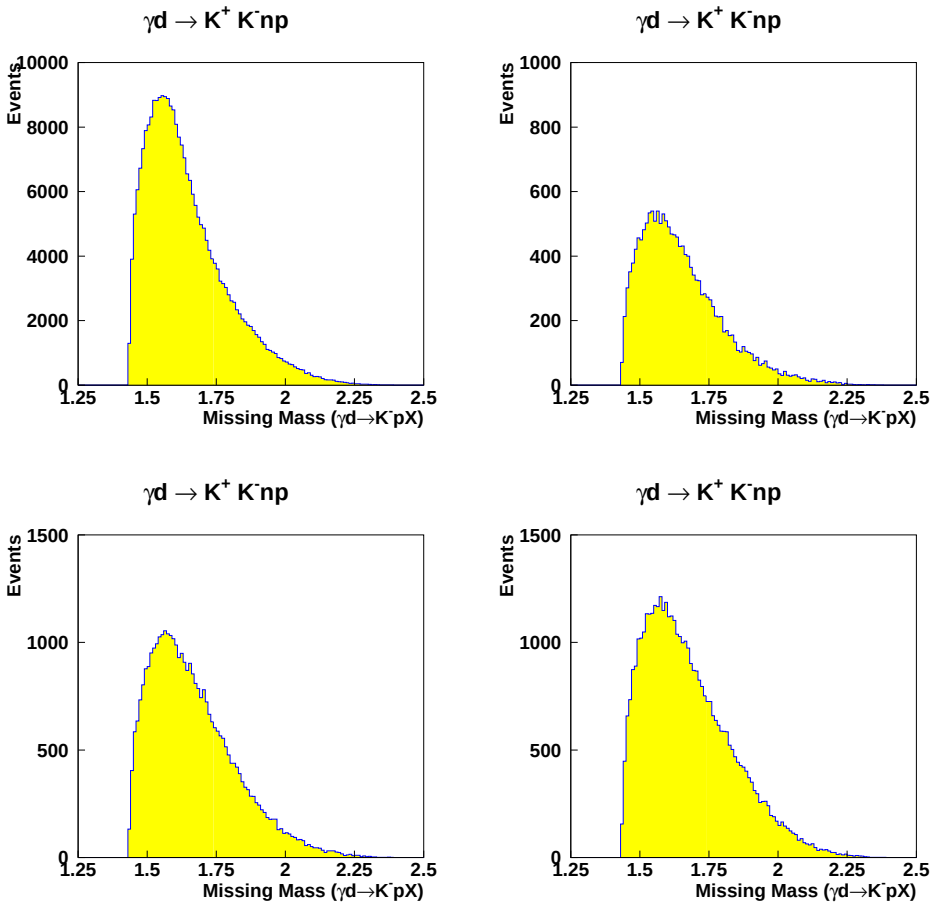

Figure 46: The K^+n invariant mass as weighted by the three different resonance in Figure 18 in the K^-n (Σ) system. The upper left is for all data, the upper right is for the $\Sigma(1580)$, the lower left is for the $\Sigma(1670)$ and the lower right is for the $\Sigma(1775)$.This reaction assumes that the K^+ scatters off the spectator proton in the reaction.

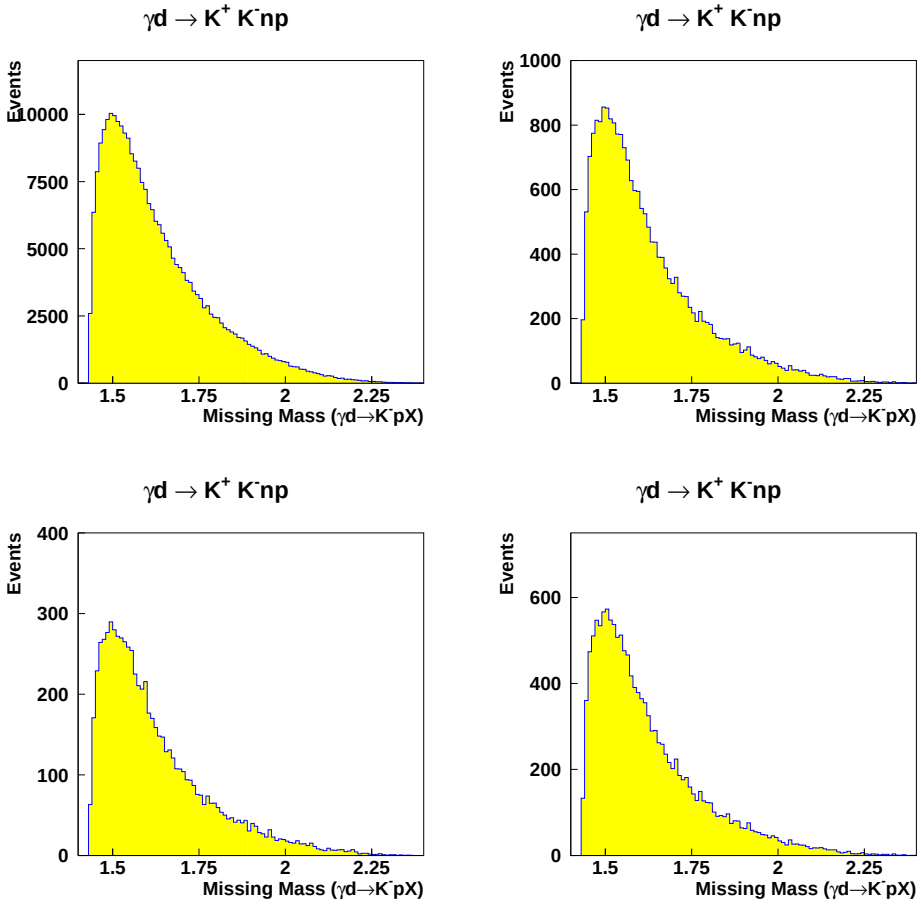

Figure 47: The K^+n invariant mass for events in which the K^- rescatters off the spectator neutron. The upper left hand figure shows all events in which the proton momentum is larger than $0.3\,GeV/c$. The upper right hand figure has all events in which the proton momentum is larger than $0.3\,GeV/c$ and the K^-p events comes from a $\Lambda(1520)$ which decays isotropically in its rest frame. The lower left figure shows the invariant mass in which the proton momentum is larger than $0.3\,GeV/c$ and the K^-p events comes from a $\Lambda(1520)$ which decays with a $\cos^2\theta$ distribution in it rest frame. The lower right hand figure shows the invariant mass in which the proton momentum is larger than $0.3\,GeV/c$ and the K^-p events comes from a $\Lambda(1520)$ which decays with a $\sin^2\theta$ distribution in it rest frame.

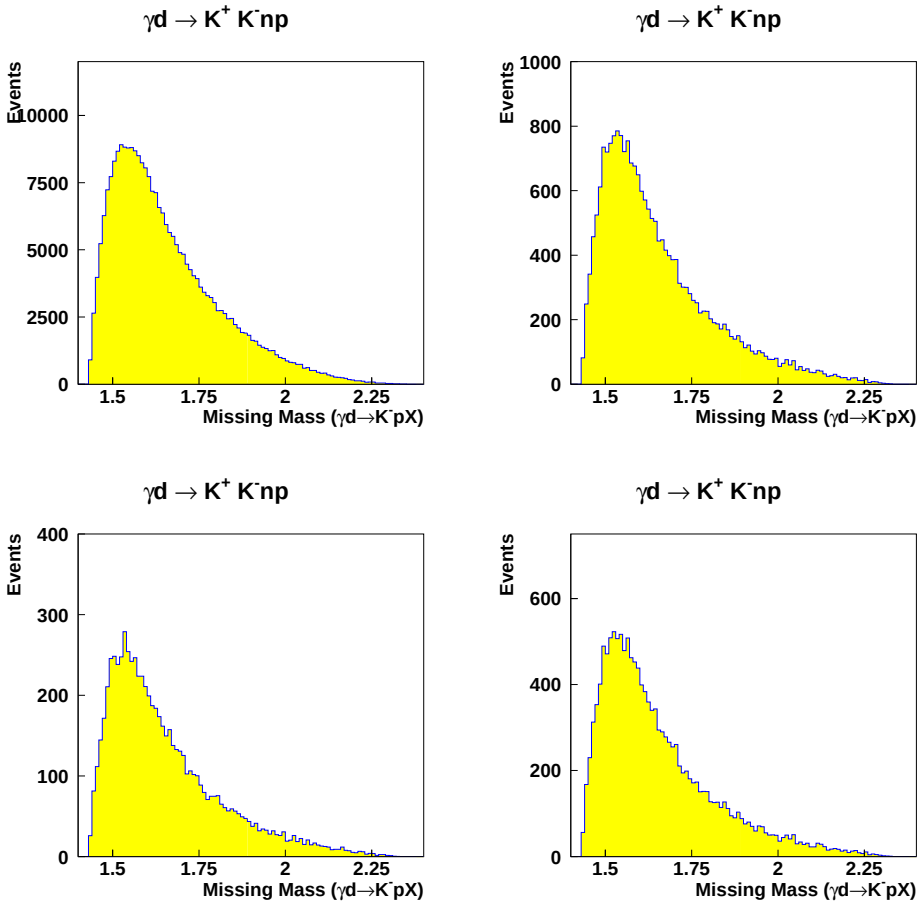

Figure 48: The K^+n invariant mass for events in which the K^+ rescatters off the spectator neutron. The upper left hand figure shows all events in which the proton momentum is larger than $0.3\,GeV/c$. The upper right hand figure has all events in which the proton momentum is larger than $0.3\,GeV/c$ and the K^-p events comes from a $\Lambda(1520)$ which decays isotropically in its rest frame. The lower left figure shows the invariant mass in which the proton momentum is larger than $0.3\,GeV/c$ and the K^-p events comes from a $\Lambda(1520)$ which decays with a $\cos^2\theta$ distribution in it rest frame. The lower right hand figure shows the invariant mass in which the proton momentum is larger than $0.3\,GeV/c$ and the K^-p events comes from a $\Lambda(1520)$ which decays with a $\sin^2\theta$ distribution in it rest frame.

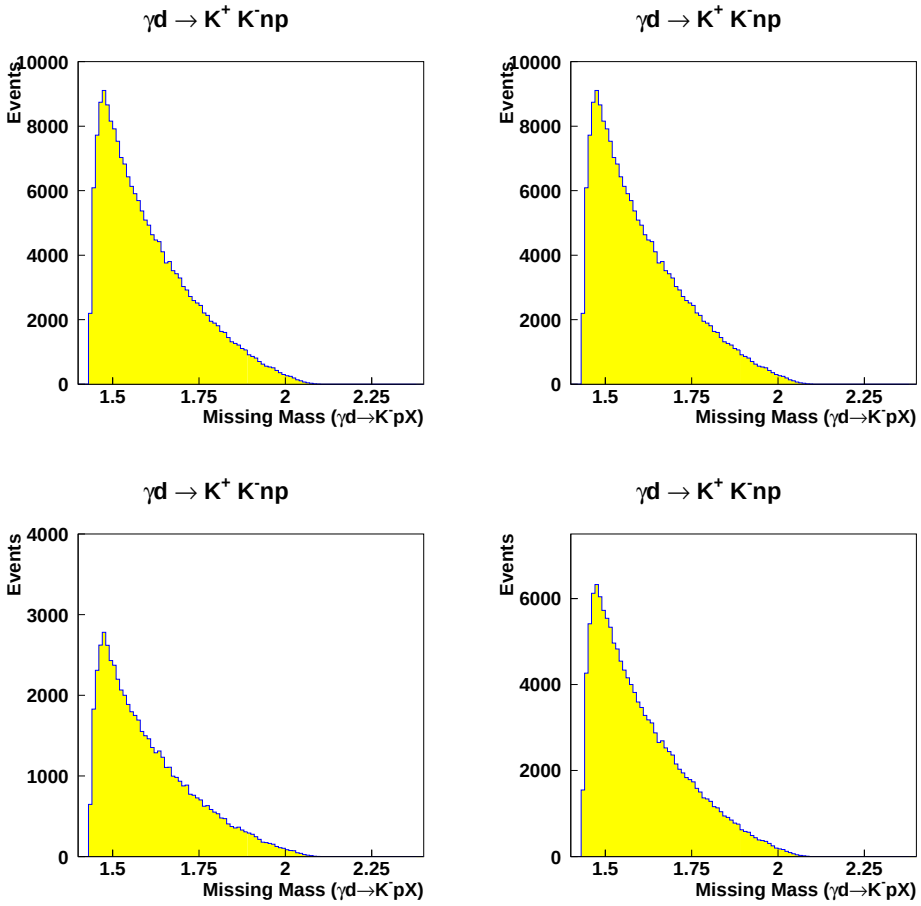

Figure 49: The K^+n invariant mass for events in which the K^- rescatters off the spectator proton. The upper left hand figure shows all events in which the proton momentum is larger than $0.3\,GeV/c$. The upper right hand figure has all events in which the proton momentum is larger than $0.3\,GeV/c$ and the K^-p events comes from a $\Lambda(1520)$ which decays isotropically in its rest frame. The lower left figure shows the invariant mass in which the proton momentum is larger than $0.3\,GeV/c$ and the K^-p events comes from a $\Lambda(1520)$ which decays with a $\cos^2\theta$ distribution in it rest frame. The lower right hand figure shows the invariant mass in which the proton momentum is larger than $0.3\,GeV/c$ and the K^-p events comes from a $\Lambda(1520)$ which decays with a $\sin^2\theta$ distribution in it rest frame.

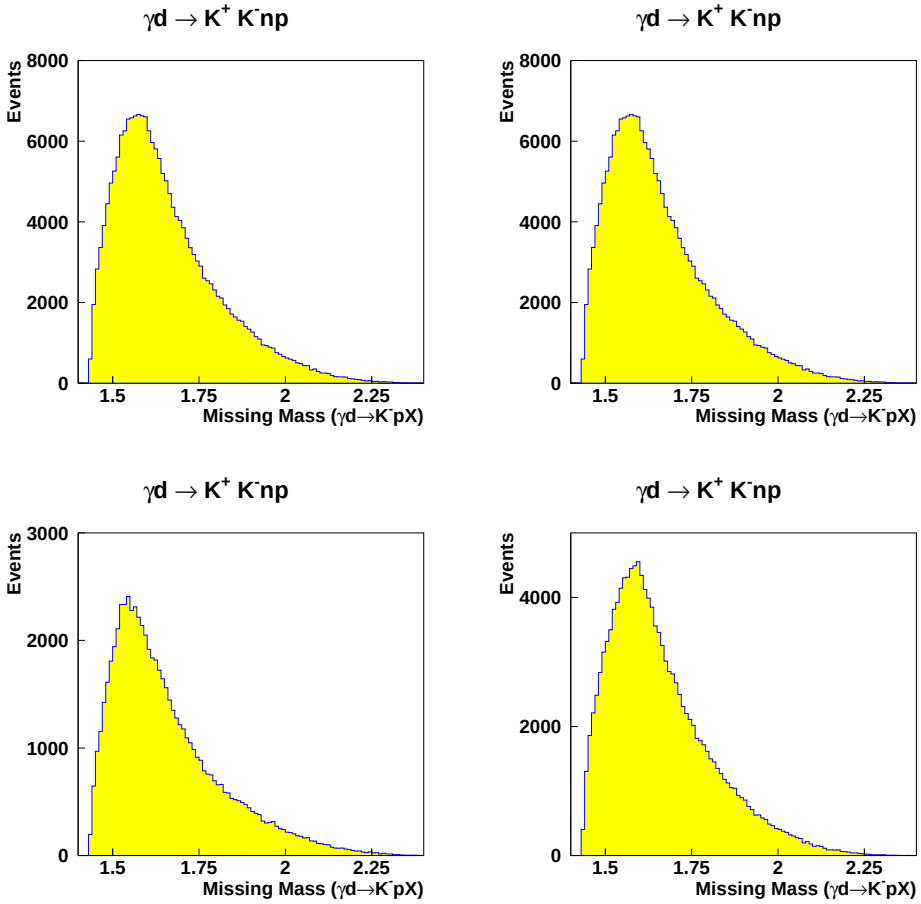

Figure 50: The K^+n invariant mass for events in which the K^+ rescatters off the spectator proton. The upper left hand figure shows all events in which the proton momentum is larger than $0.3\,GeV/c$. The upper right hand figure has all events in which the proton momentum is larger than $0.3\,GeV/c$ and the K^-p events comes from a $\Lambda(1520)$ which decays isotropically in its rest frame. The lower left figure shows the invariant mass in which the proton momentum is larger than $0.3\,GeV/c$ and the K^-p events comes from a $\Lambda(1520)$ which decays with a $\cos^2\theta$ distribution in it rest frame. The lower right hand figure shows the invariant mass in which the proton momentum is larger than $0.3\,GeV/c$ and the K^-p events comes from a $\Lambda(1520)$ which decays with a $\sin^2\theta$ distribution in it rest frame.

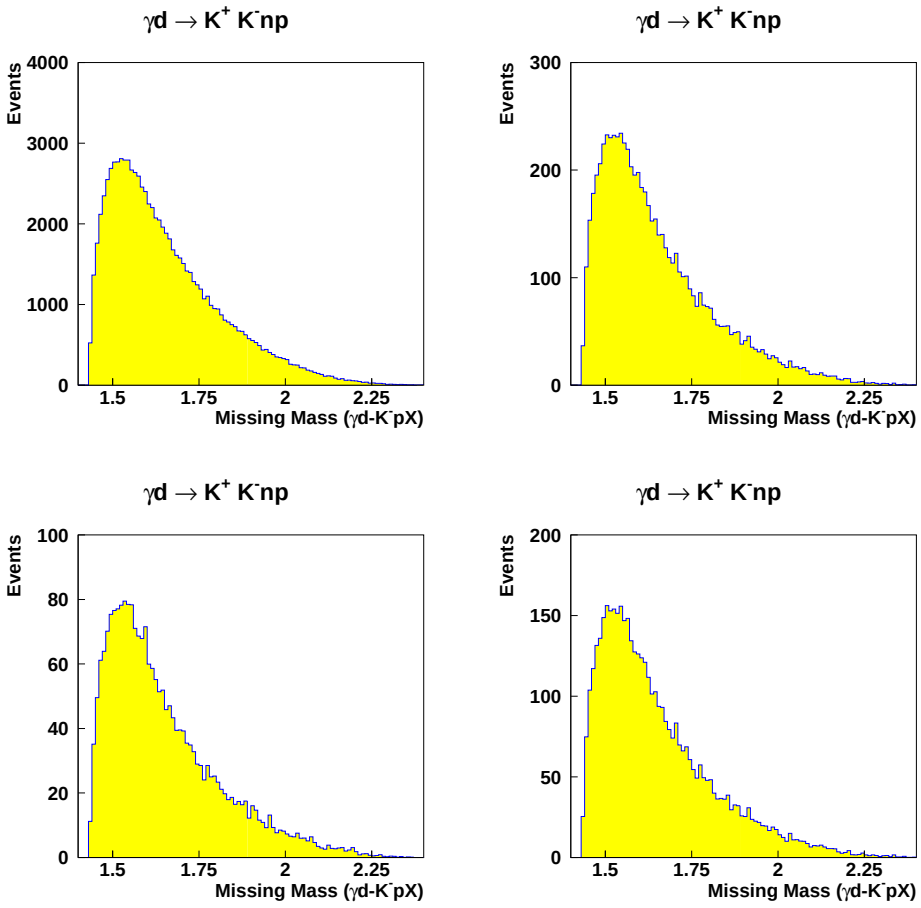

Figure 51: The K^+n invariant mass with decay probabilities applied to the K^+ assuming a $3\,m$ flight path. These events have the K^- rescattering off the spectator neutron. The upper left hand figure shows all events in which the proton momentum is larger than $0.3\,GeV/c$. The upper right hand figure has all events in which the proton momentum is larger than $0.3\,GeV/c$ and the K^-p events comes from a $\Lambda(1520)$ which decays isotropically in its rest frame. The lower left figure shows the invariant mass in which the proton momentum is larger than $0.3\,GeV/c$ and the K^-p events comes from a $\Lambda(1520)$ which decays with a $\cos^2\theta$ distribution in it rest frame. The lower right hand figure shows the invariant mass in which the proton momentum is larger than $0.3\,GeV/c$ and the K^-p events comes from a $\Lambda(1520)$ which decays with a $\sin^2\theta$ distribution in it rest frame.

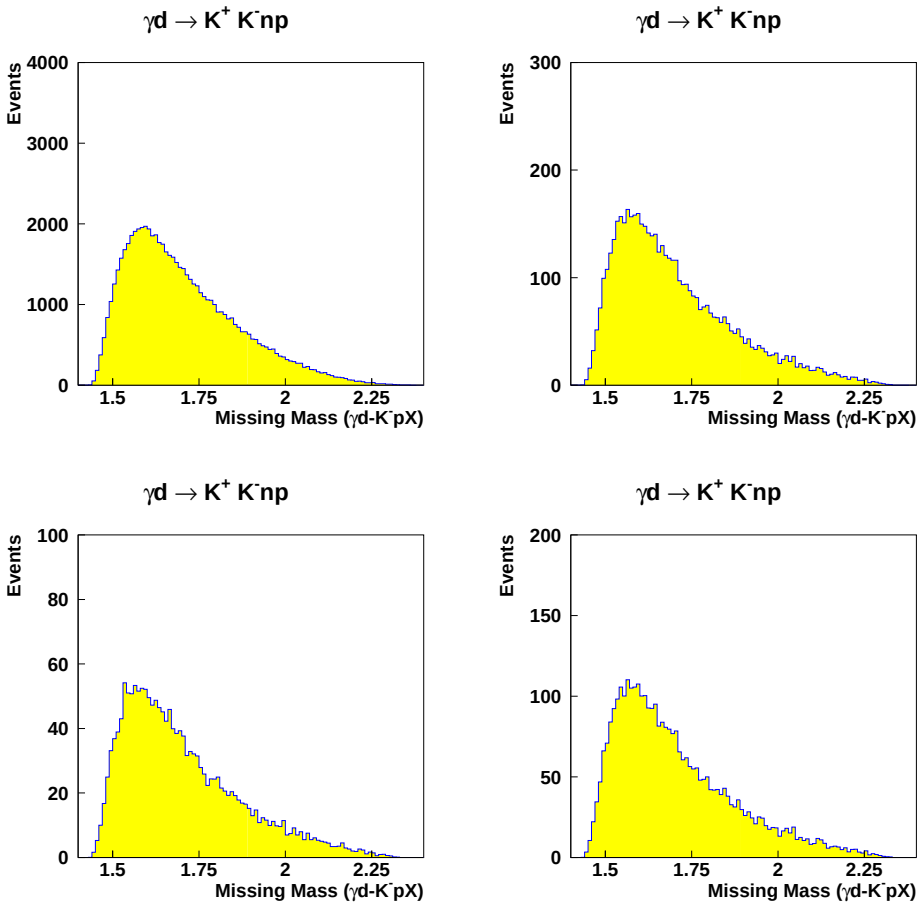

Figure 52: The K^+n invariant mass with decay probabilities applied to the K^+ assuming a $3\,m$ flight path. These events have the K^+ rescattering off the spectator neutron. The upper left hand figure shows all events in which the proton momentum is larger than $0.3\,GeV/c$. The upper right hand figure has all events in which the proton momentum is larger than $0.3\,GeV/c$ and the K^-p events comes from a $\Lambda(1520)$ which decays isotropically in its rest frame. The lower left figure shows the invariant mass in which the proton momentum is larger than $0.3\,GeV/c$ and the K^-p events comes from a $\Lambda(1520)$ which decays with a $\cos^2\theta$ distribution in it rest frame. The lower right hand figure shows the invariant mass in which the proton momentum is larger than $0.3\,GeV/c$ and the K^-p events comes from a $\Lambda(1520)$ which decays with a $\sin^2\theta$ distribution in it rest frame.

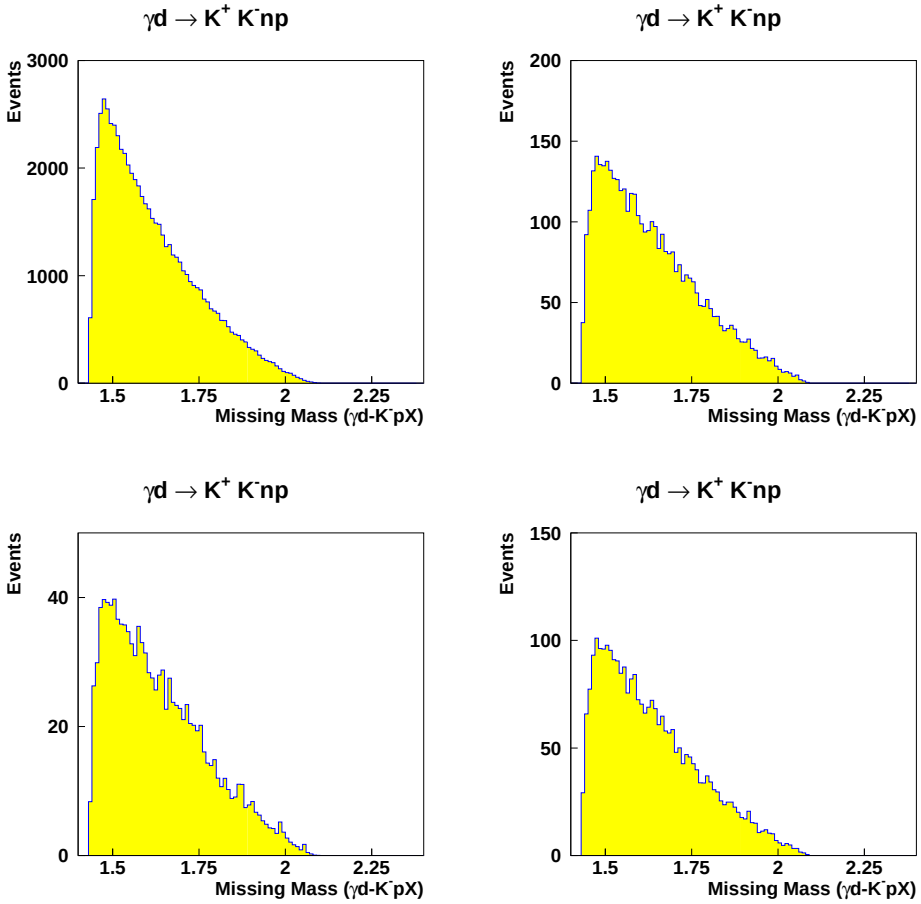

Figure 53: The K^+n invariant mass with decay probabilities applied to the K^+ assuming a $3\,m$ flight path. These events have the K^- rescattering off the spectator proton. The upper left hand figure shows all events in which the proton momentum is larger than $0.3\,GeV/c$. The upper right hand figure has all events in which the proton momentum is larger than $0.3\,GeV/c$ and the K^-n events comes from a $\Sigma(1560)$ which decays isotropically in its rest frame. The lower left figure shows the invariant mass in which the proton momentum is larger than $0.3\,GeV/c$ and the K^-p events comes from a $\Sigma(1560)$ which decays with a $\cos^2\theta$ distribution in it rest frame. The lower right hand figure shows the invariant mass in which the proton momentum is larger than $0.3\,GeV/c$ and the K^-p events comes from a $\Sigma(15260)$ which decays with a $\sin^2\theta$ distribution in it rest frame.

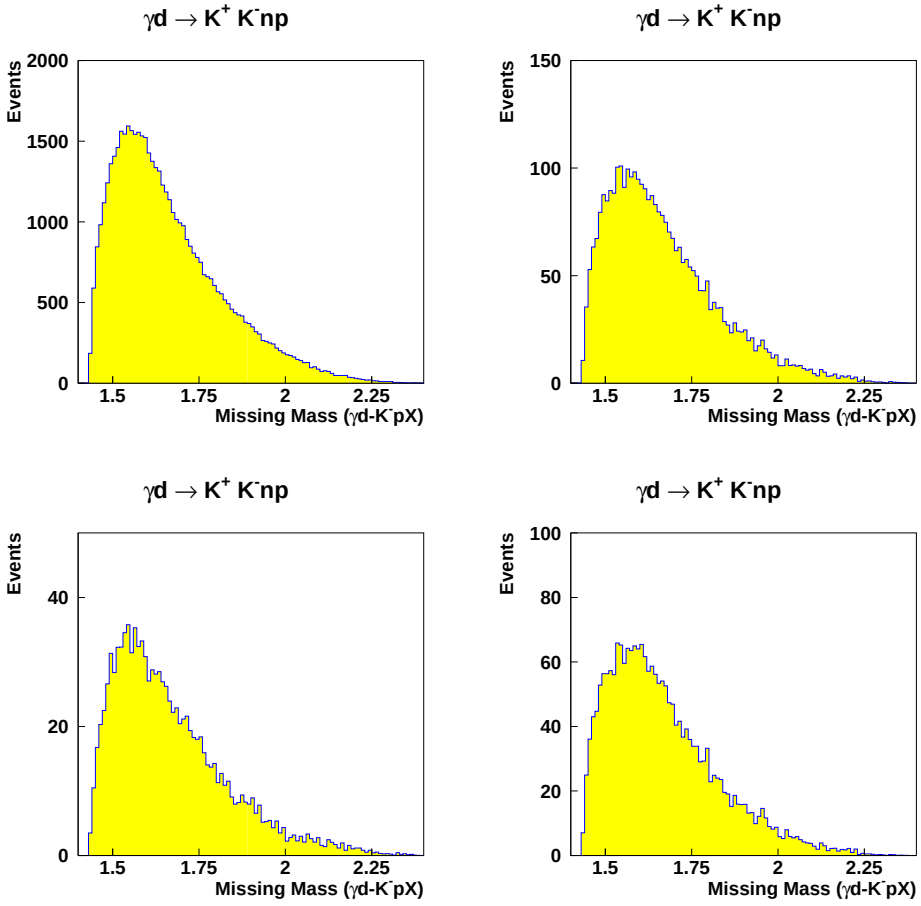

Figure 54: The K^+n invariant mass with decay probabilities applied to the K^+ assuming a $3\,m$ flight path. These events have the K^+ rescattering off the spectator proton. The upper left hand figure shows all events in which the proton momentum is larger than $0.3\,GeV/c$. The upper right hand figure has all events in which the proton momentum is larger than $0.3\,GeV/c$ and the K^-n events comes from a $\Sigma(1560)$ which decays isotropically in its rest frame. The lower left figure shows the invariant mass in which the proton momentum is larger than $0.3\,GeV/c$ and the K^-p events comes from a $\Sigma(1560)$ which decays with a $\cos^2\theta$ distribution in it rest frame. The lower right hand figure shows the invariant mass in which the proton momentum is larger than $0.3\,GeV/c$ and the K^-p events comes from a $\Sigma(1560)$ which decays with a $\sin^2\theta$ distribution in it rest frame.

9 Summary and Conclusions

We have examined events from the reaction $\gamma d \rightarrow npK^+K^-$ in which one of the final-state nucleons starts out as a spectator at rest, but acquires a final momentum due to rescattering of one of the kaons. Resonance weights have been applied to the K^-N and K^+K^- systems, as well as decay and production angular distributions. It does not seem possible to generate peaks narrower than about $0.040\,GeV$ in the K^+n spectrum through reflections and cuts.

References

[1] The Durham Database Group, *HEPDATA, The Durham HEP Databases*, `http://durpdg.dur.ac.uk/HEPDATA/`.

[2] The Center for Nuclear Studies Data Analysis Center, SAID, `http://gwdac.phys.gwu.edu/`.

[3] John S. Hyslop, Richard A. Arndt, L. David Roper and Ron L. Workman, **Partial-wave analysis of K^+-nucleon scattering**, Phys. Rev. D**46**, 961, (1992).

[4] Damerell, *et al.*, Nucl. Phys. B**94**, 374, (1975).

[5] Damerell, *et al.*, Nucl. Phys. B**129**, 397, (1977).

[6] The CERN Program Library, W515, `http://wwwasd.web.cern.ch/wwwasd/cernlib/mc/genb`

[7] K. Hagiwara *et al.*, Review of Particle Physics, Phys. Rev. D**66**, 1, (2002).

List of Figures

1 Scattering parameters. 2
2 $d\sigma/d\Omega$ for $K^+n \to K_Sp$. 3
3 $d\sigma/d\Omega$ for $K^+n \to K^+n$. 4
4 $d\sigma/d\Omega$ for $K^+n \to K^+n$. 5
5 $d\sigma/d\Omega$ for $K^+n \to K^+n$. 6
6 $d\sigma/d\Omega$ for $K^-n \to K^-n$. 7
7 $d\sigma/d\Omega$ for $K^-n \to K^-n$. 8
8 $d\sigma/d\Omega$ for $K^-n \to K^-n$. 9
9 $d\sigma/d\Omega$ for $K^-n \to K^-n$. 10
10 S-wave K^+n phase shifts. 12
11 P-wave K^+n phase shifts. 12
12 P-wave K^+n phase shifts. 13
13 Resonance phase shift 13
14 Resonance phase shift 14
15 Scattering processes. 16
16 Photon energy spectrum 16
17 t and s. 17
18 Λ resonances. 18
19 Σ resonances. 19
20 Baryon momentum. 20
21 K^+K^- resonances. 21
22 t versus $m(K^+n$. 24
23 $m(K^-p$ versus $m(K^+n$. 25
24 $\cos\theta_{K^-N}$ versus $m(K^+n$. 26
25 s versus $m(K^+n$. 27
26 $\cos\theta_{KN}$ versus $m(K^+n$. 28
27 Proton momentum versus $m(K^+n$. 29
28 Neutron momentum versus $m(K^+n$. 30
29 K^- momentum versus $m(K^+n$. 31
30 Proton momentum versus $m(K^+n$. 32
31 θ_p versus $m(K^+n$. 33
32 θ_{K^-} versus $m(K^+n$. 34
33 θ_{K^+} versus $m(K^+n$. 35
34 m_{KK} versus $m(K^+n$. 36
35 t versus $m(K^+n$. 37
36 Kaon time of flights. 38

37 Kaon time of flights. 39
38 Kaon time of flights. 39
39 Kaon time of flights. 40
40 K^+n mass with $\phi \rightarrow K^+K^-$. 42
41 K^+n mass with $\phi \rightarrow K^+K^-$. 43
42 K^+n mass with $\phi \rightarrow K^+K^-$. 44
43 K^+n mass with Λ resonances. 46
44 K^+n mass with Λ resonances. 47
45 K^+n mass with Σ^- resonances. 48
46 K^+n mass with Σ^- resonances. 49
47 K^+n mass with $p_p \geq 0.3$. 50
48 K^+n mass with $p_p \geq 0.3$. 51
49 K^+n mass with $p_p \geq 0.3$. 52
50 K^+n mass with $p_p \geq 0.3$. 53
51 K^+n mass with decays. 54
52 K^+n mass with decays. 55
53 K^+n mass with decays. 56
54 K^+n mass with decays. 57